Design of a SystemView Simulation of a Stepped Frequency Continuous Wave Ground Penetrating Radar

Prepared By
Andile Mngadi
Final year Electrical Engineering Student
University of Cape Town

This thesis is submitted to the Department of Electrical Engineering, University of Cape Town, in partial fulfilment of the requirements for the degree of Bachelor of Science in Engineering.

Cape Town, October 2004

25th October 2004

Document No: rrsg:00

Approval

	Name	*Designation*	*Affiliation*	*Date*	*Signature*
Submitted by					
Reviewed by					
Accepted by					
Approved by					
Approved by					
Approved by					

Document History

Revision	*Date of Issue*	*RRSG Number*	*Comments*
A	25th October 2004	rrsg:00	

Document Software

	Package	*Version*	*Filename*
Text Processor	LyX	1.3.4	

Company Details

Name	Radar Remote Sensing Group, University of Cape Town
Physical Address	Department of Electrical Engineering, Robert Menzies Room 609, University of Cape Town, Upper Campus, Rondebosch
Postal Address	Department of Electrical Engineering, Robert Menzies Room 609, University of Cape Town, Private Bag, Rondebosch 7701, South Africa
Telephone	+27 (0)21 650 2799
Fax	+27 (0)21 650 3465
Email	mikings@ebe.uct.ac.za

Declaration

I declare that this thesis is my own, unaided work. It is submitted for the degree of Bachelor of Science in Engineering at the University of Cape Town. It has not been submitted before for any degree or examination in any other university.

Signature of Author.....

Department of Electrical Engineering,

Cape Town , October 2004

Acknowledgements

I would like to thank my supervisor, Professor Michael Inggs, for his continual support and guidance throughout the project period. Without his assistance, completion of this project would not have been possible.

For financially assistance, I am grateful to Denel Pty (Ltd) for their financial assistance throughout these years.

Thanks to Busisiwe Paliso for keeping me sane, and her support and patience. Many thanks for always lending a helping hand and keeping me up to date.

To Georgie Goerge, I am thankful for the trouble he went through helping me with simulating the stepped frequency waveform.

Thanks to Richard Lord, and Andrew Wilkinson for all their support and patience.

Finally I wish to thank the members of the Radar and Remote Sensing Group at University of Cape Town for their support whenever possible.

To my family.

Terms of Reference

The following instructions were given to me by Professor Michael Inggs on the 21st July 2004:

- Develop a SystemView simulator of a stepped frequency radar system
- The number of frequencies, integration strategies shall be close the existing ground penetrating radar (GPR) systems
- Real components imperfections are to be given.
- Implement an adaptable system that covers an arbitrary start and stop frequency, use start frequency of 1MHz and stop frequency of 100MHz.
- The frequency step size must also be adaptable, typically to fit with the FFT radix 2 algorithm, use 32, 64, or 128 for the number of frequency steps.
- Assume a constant permittivity $\varepsilon_r = 6$ for the propagation medium, assuming soil.
- Assumptions made during the simulation must be clearly stated in the report.

The following instructions were given for the comparison of the stepped frequency radar system with the Impulse GPR radar system:

- The gain of both the transmit and receive antenna must be set to equal to one for both systems.
- The propagation medium must be a straight attenuative loss of 10dB and zero time delay to reduce simulation time.
- The number of frequency steps must be 64 and 50 range profiles must be taken per second.
- Use an IF filter with a bandwidth of 100kHz. The ADC must be a 14bit .
- The ADC must take 128 samples while the signal is dwelling on each frequency. These samples are averaged to produce a single IQ value.

- The transmit signal power is 10 dBm and the receiver noise figure is 5dB.

The working simulation scripts, test results and the final report are to be submitted on the 19th October 2004.

Synopsis

Research into stepped frequency continuous wave ground penetrating radar (SFCW GPR) has been carried out since 1990 at UCT. However, this is the first thesis that discusses the simulation of SFCW GPR using SystemView. SystemView is a time domain system simulator environment for the design and analysis of engineering, mathematical and scientific systems. Frequency domain analysis of the signals in SystemView analysis window is also possible.

A SFCW GPR system was simulated in SystemView. Various transmitter configuration were discussed and the variable parameter configuration was found most suitable and therefore was used for the simulation. The variable parameter configuration was found most suitable because of its easily adaptable characteristics. When the variable parameter configuration was used, it was found that transmitter frequency can be made to cover any arbitrary frequency range, by a simple mouse click. Also the frequency stepsize and the number of frequency steps were automated when the increment value was changed, in this configuration. For the simulation, the transmitter covered the 1-100 MHz frequency band with the transmitter power of 10 mW.

The propagation medium, assumed soil with a constant relative permittivity, was simulated from a simple attenuator. For a constant relative permittivity, it was found that there is a linear relationship between the attenuation and frequency. Therefore, the real ground characteristics were simulated based on the attenuation versus frequency relationship. A heterodyne receiver architecture for the 1-100 MHz signal was simulated, to mix the signal to an IF of 1 MHz and demodulate the signal. Digitisation was performed by a 14 bit quantiser with a 2 V voltage span. The mean noise value was found important for signal averaging in post processing. Signal processing was not satisfactory, even though the performance was better than the Impulse GPR system. Zero-padding the range profile in signal processing improved the high range resolution profile. Stacking was found difficult in SystemView for the SFCW GPR, the machine ran out of memory when stacking was attempted. Therefore the alternative was found to be Matlab. This was left out for future work.

The system performance was tested by comparing the SFCW GPR to the Impulse GPR. In terms of the dynamic range, SNR, and transmit power, the SFCW performance was found better. Advanced signal processing methods were recommended for the SFCW to further shows its capabilities over the Impulse GPR. Other recommendations include medium and antenna future work.

List of Symbols

A	Amplitude [m]
B	Bandwidth [Hz]
B_{tot}	Total radar bandwidth [Hz]
c	Speed of light [m/s]
F	Noise figure [dB]
f	Frequency [Hz]
f_{ad}	A/D sampling frequency [Hz]
f_b	Beat frequency [Hz]
f_c	Radar centre transmit frequency [Hz]
f_L	Lower frequency [Hz]
f_0	Start frequency
f_s	Frequency shift
f_U	Upper frequency [Hz]
Δf	Frequency step size [Hz]
G_a	Antenna gain
G_t	Transmitter antenna gain
G_r	Receiver antenna gain
H_i	Range profile transfer function
i	A positive integer
n	Number of frequency steps
N	Number of pulses or signals
N_0	Output noise power [dBm]
P_{ave}	Average transmitted power [W]
P_{peak}	Peak transmitted power [W]
P_1	1 dB compression point [dB]
P_3	Third-order intercept point [dBm]
R	Range [m]
R_{max}	Maximum range [m]
R_{unam}	Maximum unambiguous range [m]

S_0	Output signal power [dBm]
T_{dwell}	Dwell time per frequency
t	Time [s]
T	Signal period [s]
t_t	Travel time [s]
Δt	Two-way time resolution [s]
ϕ_i	Phase of the signal i [rad]
$\Delta\phi$	Phase difference [rad]
Δz	Range bin spacing [m]
ω	Angular frequency [rad/s]
λ	Wavelength [m]

Nomenclature

A/D Analogue to Digital converter

Beamwidth The angular width of a slice through the mainlobe of the radiation pattern of an antenna in the horizontal, vertical or other plane.

BHR Bore Hole Radar

Burst Set of frequencies required to produce a synthetic range profile.

Coherence A continuity or consistency in the phase of successive radar pulses.

CPI Coherent Processing Interval

CW Continuous Wave

DC Direct current

EM Electromagnetic

FFT Fast Fourier Transform

FM Frequency Modulation.

FMCW Frequency Modulation Continuous Wave.

GPR Ground Penetrating Radar.

I In-phase

IDFT Inverse Discrete Fourier Transform

IF Intermediate Frequency

IFFT Inverse Fast Fourier Transform.

LNA Low Noise Amplifier

LO Local Oscillator

Narrowband Describes radar systems that transmit and receive waveforms with instantaneous bandwidths less than 1 percent of centre frequency (Taylor 2001).

Profile Contour of the target outline which is deduced from reflected signals in a radar system.

Q Quadrature

Radar Radar Detection and Ranging.

Range The radial distance from a radar to the target.

RF Radio Frequency

RFI Radio Frequency Interference.

RRSG Radar Remote Sensing Group (UCT).

RX Receiver

SFCW Stepped Frequency Continuous Waveform

SFGPR Stepped Frequency Ground Penetrating Radar

SNR Signal to noise ratio

SRP Synthetic Range Profile.

SV SystemView

TX Transmit

Wideband Describes radar systems that transmit and receive waveforms with instantaneous bandwidths between 1 percent and 25 percent of centre frequency (Taylor 2001)

Contents

List of Figures

List of Tables

Chapter 1

Introduction

1.1 Background to Study

It is essential to understand today's scope of ground penetrating radar systems. Ground penetrating radar (GPR) is simply a technology that can *see* underground. A ground penetrating radar sensor is needed to provide information which will allow the user to extract the geometrical and physical properties of the targets that are buried or located beneath a particular surface [1].

In GPR radars, the more information the sensor captures, the greater the chance of solving the problem of locating, detection and identifying subsurface features and then possibly relate the data to some physical phenomena. However, the information captured from the target is limited by the properties of the media, the dielectric permittivity and conductivity (σ, ε) . Most media will show increased losses with increased frequency. This forces a practical limit on the maximum bandwidth of the transmit waveform. Hence, in deciding what signal to transmit, one must consider a waveform that will maximize the information returned from the target.

Various researchers [1, 2, 3] have shown that the Stepped Frequency Continuous Wave (SFCW) modulation offers greater bandwidth, transmit power, spectral control, sensitivity and dynamic range than equivalent modulation systems. This is the motivation behind this thesis project.

1.2 Problems to be Investigated

The following problems will be investigated in this report:

1. The use of stepped frequency waveforms to obtain larger total radar bandwidth and eventually improve the range resolution, and

2. The performance of a stepped frequency continuous wave ground penetrating radar compared to an impulse ground penetrating radar.

3. Stacking the radar signals to improve the signal to noise ratio.

The two systems will be simulated and basis of comparison are as stipulated in the terms of reference. The simulation of the stepped frequency system will be done by the writer and discussed in this report. The reader is referred to a thesis by Guma et al [4] for the simulation of the Impulse ground penetrating radar system.

1.3 Thesis Objectives

The three main problems to investigated quantify the thesis objectives as to:

1. Create a SystemView simulation of a stepped frequency continuous wave ground penetrating radar

2. Obtain high range resolution profiles of the simulated SFCW GPR radar system

3. Compare the performance of the SFCW system to that of the impulse GPR with and without stacking.

1.4 Scope and Limit of the study

This thesis describes the design of a simulation of a Stepped Frequency Continuous Wave (SFCW) Ground Penetrating Radar(GPR), using SystemView. The scope of the thesis further includes comparison of Stepped-Frequency GPR radar with the impulse GPR radar system. The scope does not however include the simulation of the impulse radar system. The simulation of the impulse ground penetrating radar system is tackled separately as a thesis project by a fellow member of the Radar and Remote Sensing Group (RRSG) at the University of Cape Town. Also because of time constraints, the simulation of real systems of the radar, are kept simple without being simplistic.

1.5 About SystemView^{TM}

Chapter 1 of the SystemView's user guide manual, which can be obtained from the help menu of SystemView (SV), describes SystemView as follows. "SystemView is a comprehensive dynamic

system analysis environment for the design and simulation of engineering or scientific systems. From analog or digital signal processing, filter design, control systems, and communication systems to general mathematical systems modeling, SystemView provides a sophisticated analysis engine".

SystemView is a time domain simulator, however, the powerful sink calculator of SystemView allows frequency domain analysis of the signals. In SystemView large systems can be easily simplified by defining groups of tokens as a MetaSystem. A MetaSystem allows a single token to represent a complete system or subsystem. A simple mouse click opens a window showing the complete subsystem contained in the MetaSystem.

1.6 Radar Background Theory

1.6.1 Definition

RADAR stands for RAdio Detection And Ranging. This acronym is falling short of defining the scope of today's electromagnetic surveillance. Radar now includes other important functions in addition to detection and ranging. Modern high resolution radars provide ground mapping, and, more recently, target recognition and imaging. Nonetheless, the basic equation governing the range at which the target can be detected remains fundamental to modern radar design [5].

Most radars developed in the past were pulsed radars. These radars have a power and bandwidth limitation. In overcoming the power and bandwidth limitations of the simple pulsed radar, alternative waveforms were developed which allow mean power through the transmission of longer pulses for extending the range capability, yet retaining wide bandwidth for high resolution. Radar systems generating these waveforms are called *wideband* or *high resolution*, where fractional bandwidth of up to 20% are possible. Stepped Frequency GPR radars are one such radar systems.

1.6.2 The Radar Equation

Radars operate by transmitting power P_t, which is the mean radio frequency (RF) power in watts from a transmitting antenna, which has an *antenna gain* of G_t. The *power density* (in Watts per square metres) of a transmitted signal incident on a target at range R is $\frac{P_t G_t}{4\pi R^2}$. The target scatters incident power in all directions including back to the radar. The scattered power from a target of *radar cross section* σ_t (in square metres) is $\frac{P_t G_t \sigma}{4\pi R^2}$. The resulting reflected power density at the radar receiver antenna is $\frac{P_t G_t \sigma}{4\pi R^2} \times \frac{1}{4\pi R^2} \times \frac{1}{L}$. The factor "L" compensates for the "loss " in the signal power during propagation to and from the target. The receiver antenna has an *effective aperture* of $G_r \frac{\lambda^2}{4\pi}$ square metres, where G_r is the *receiver antenna gain,* and λ is the *propagation wavelength* ($\lambda = c/f$

in free space, where f is the frequency). The received signal power P_r from the point target measured at the radar is given by the equation below*:*

$$P_r = \frac{P_t G_t G_r \lambda^2 \sigma_t}{(4\pi)^3 R^4 L}$$

This equation is known as the *radar equation* [5]. The maximum range of the radar can be calculated by

$$R_{max} = \left[\frac{P_t G_t G_r \lambda^2 \sigma_t}{(4\pi)^3 F k T_0 B_n (SNR) L} \right]^{1/4}$$

Most of the parameters on the right hand side of the above equation can be controlled by the radar designer, who is most concerned with finding the most appropriate values of the parameters to suit the particular application. The reader is referred to [2, 5, 6, 7] for a detailed discussion and derivation of this principle. Important equations governing stepped-frequency waveforms and ground penetrating radars are discussed in the next chapter. The radar equation mentioned above will be modified appropriately for ground penetrating radar applications.

1.7 Plan of Development

This chapter is an overview of the thesis report. It has presented the thesis objectives, the thesis scope and a brief definition of the radar term and the fundamental range equation which is the backbone of radar system design. Also presented is the problems that GPR systems are facing, which is the motivation for undergoing this study. We now give an overview of the next chapters of the thesis report.

Chapter 2 starts with a summarised description of stepped frequency continuous wave (SFCW) radars. The chapter briefly describes how these SF waveforms are attained and how they are used to obtain distance information of the target. In section 2.3, the writer describes how SF waveforms are used in GPR radars. This section describes in simple terms how a SFGPR radar operate and how a high range-resolution profile is obtained using SF waveforms. A simple manner for the modelling of transmitted waveforms in a generally lossy medium is introduced and simple equations relating to the unambiguous range and the range-resolution are also introduced. The equations are used to introduce the simulation requirements in terms of the system bandwidth, the frequency step size, the number of frequency steps and the relative permittivity of the propagation medium. The propagation medium and the receiver specifications are also presented and further dicussed in chapters 4 and 5 respectively. The chapter ends with an extract from Noon [2] of the distinction between SFCW and FMCW. FMCW

measure the travel time of a signal directly from the difference in frequency (that is, the beat frequency, $f_b = Bt_t/T_{dwell}$, where t_t is the travel time of the signal and T_{dwell} is the dwell time) between the receiver and reference paths. The IDFT is used to transform the different beat frequencies of the targets to a time profile where the travel times to the targets are well resolved according to the FMCW bandwidth. On the other hand, the stepped-frequency radar measures the travel time of the reflected signals by measuring the phase difference between the receiver and reference paths at each frequency. In-phase and quadrature samples must be taken at each frequency step to measure the phase.

The transmitter is discussed in Chapter 3. The transmitter is the heart of a continuous wave system, since the coherency of the transmit-receive signals determines the accuracy of the measurements [8] . This chapter discusses the simulation design of the transmitter of a stepped frequency ground penetrating radar and its performance. It was noted that are numerous ways of simulating a stepped frequency radar transmitter in SystemView. Two of these methods are mentioned in passing in this chapter, however emphasis is given to the simulation that was chosen for this project . The reader must note that the design used for the transmitter is not similar to the one described in most textbooks [5, 6, 7, 9], but rather serves the purpose. In SystemView there are ways in which most of the practical design requirements (for instance, the actual frequency synthesizer block in the transmitter) can be eliminated without losing the essence of the simulation. In the simulation of the transmitter, the main interest lies in the output of the transmitter.

The simulation of the transmitter can be summarised as follows. A stepped frequency continuous wave transmitter was simulated. It has a start and stop frequency of 1 MHz and 100 MHz respectively. Each frequency is transmitted for a millisecond, this is what we call the dwell time per frequency. The number of frequency steps taken is *n* equal to 32 for a frequency stepsize equals of 3.2 MHz. Both the number of frequency steps taken and the frequency stepsize are easily adaptable in SystemView. This means to change the number of steps and the stepsize simply requires retyping the correct values in SystemView. This is one major advantage of using the Token Parameter Variation method, instead of using the two methods described in subsection 3.3.1 and 3.3.2. The maximum transmitted frequency sets the sample rate of the transmitter system to 400 MHz. The performance of the transmitter was evaluated by viewing the spectrum of the transmitted waveform. As required by the specification of the simulation the transmitter power was 10 dBm, which is equivalent to 10 mW. The spectral purity of the transmitter was justified by the signal to noise ratio of 110 dB at the output of the transmitter. Phase noise was observed at the point where each frequency changes. Even though it does not satisfy the definition of frequency jitter, it was observed that not all signals have power levels at 10 dBm. This however was regarded as the only frequency jitter. The little spikes at the end of each dwell time caused phase noise. This is however not frequency jitter see figure 3.3. The frequency accuracy of the transmitted frequencies was also observed from the spectrum plots and each signal was seen to be located at its transmit frequency.

Chapter 4 discusses the simulation of the propagation medium in which the transmitted signal prop-

agates and the target is located. This chapter can be summarised as follows. From the theory on ground penetrating radar systems, it is generally difficult to calculate the penetration depth as it is a complex function of the ground characteristics. Therefore, two propagation medium simulations were discussed, depicting both the simple ground model and the real ground characteristics. The first medium was a straight attenuative medium with 10 dB loss. The second simulation of the medium attempts to simulate the real behavior of ground characteristics. The second simulation was based on the theory investigated by Noon et al [2] , that there is relationship between the attenuation and the frequency for a constant relative permittivity ε_r . An attenuation versus frequency curve (4.3) can be simulated using filter models in SystemView to characterise this behaviour of the propagation medium.

Chapter 5 starts with a brief summary of receiver architectures that are available to the radar design engineer. The reasons for the preferred architecture for a SFCW radar are explained. Section 5.3 discusses in great detail the simulation of the heterodyne receiver architecture. Each stage (RF stage, IF stage and the demodulation stage) of the receiver simulation is discussed independently, and the selection of the components that were used is briefed. The chapter ends with a section that shows the performance of the receiver system. The performance of the receiver system was based on the output SNR, the receiver dynamic range, and the minimum detectable signal (MDS). To avoid intermodulation distortion, a diagram showing the noise and the signal power levels through the stages of the receiver is included. The diagram ensures that P_1 and P_3 are not exceeded.

Chapter 6 presents the results of the final simulated SFCW GPR system. In chapters 3, 4, and 5 the performance of the transmitter, the medium and the receiver were discussed and results with regard to their performance were shown. For the transmitter, its performance is investigated in section 3.6. The propagation medium performance is shown in section 4.4. The receiver performance is tested in section 5.4. Therefore those results are not repeated in this chapter. This chapter mainly presents the signal processing results. Signal processing was done in Matlab. Appendix D shows the programming code that was used to generate the range profile from the data of the quantiser. The system was tested by measuring the response for various attenuators and plotting the range profiles for each attenuation. This means, the system is tested for different soil types characterised by the attenuation. The results are discussed in terms of the range resolution and the maximum range to the target. The concept of stacking is discussed and the effects it has on the signal to noise ratio. Further implications of running multiple waveforms and lopping the simulation are shown.

The comparison of the SFCW GPR to the Impulse GPR system is also discussed in Chapter 6. For comparison purposes, both the Impulse and SFGPR radar systems were modified to have the same parameters. The modification that was made to the existing system is described in section 6.2. Range profiles of the two system are discussed in section 6.5. The last section briefly summarise the performance of the SFCW GPR compared to the Impulse GPR. A brief discussion on how the number of frequency steps influence the performance of the SFCW GPR ends the chapter

Conclusion and Recommendations on the performance of the simulation system are made in chapter 7. The expereinced gained in this thesis is used to make recommendations on the future work and improvements that can be done to the SFCW GPR system simulated.

Chapter 2

Literature Review

2.1 Introduction

High range resolution has many advantages in radar. Apart from providing the ability to resolve closely spaced targets in range, it improves the range accuracy, reduces the amount of clutter within the resolution cell, reduces multi path, provides high-resolution range profiles, and aids in target-classification [9]. High range resolution techniques can be grouped in three main categories: impulse, conventional pulse compression, and frequency-step. Bandwith is achieved in a different manner in each category. In this report the writer investigates frequency-step continuous wave radars. Radars employing a stepped frequency continuous waveform increase the frequency of successive signals linearly in discrete steps.

This chapter starts with a summarised description of stepped frequency continuous wave (SFCW) radars. The chapter briefly describes how these SF waveforms are attained and how they are used to obtain distance information of the target. In section 2.3, the writer describes how SF waveforms are used in GPR radars. This section describes in simple terms how a SFGPR radar operate and how a high range-resolution profile is obtained using SF waveforms. A simple manner for the modelling of transmitted waveforms in a generally lossy medium is introduced and simple equations relating to the unambiguous range and the range-resolution are also introduced. The equations are used to introduce the simulation requirements in terms of the system bandwidth, the frequency step size, the number of frequency steps and the relative permittivity of the propagation medium. The propagation medium and the receiver specifications are also presented and further dicussed in chapters 4 and 5 respectively. The chapter ends with an extract from Noon [2] of the distinction between SFCW and FMCW.

2.2 Stepped Frequency Continuous Wave Radar

Frequency-stepping is a modulation technique used to increase the total bandwidth of the radar. In stepped frequency radars, the frequency of each signal in the waveform is linearly increased in discrete frequency steps, by a fixed frequency step. Stepped frequency continuous waves are different from stepped frequency pulses see the two theses by Langman [1] and Lord [1] . In this thesis investigate SFCW, hence the use of the word signal rather than pulse.

The waveform for a stepped frequency continuous wave radar consists of a group of *N* coherent signals whose frequencies are increased from signal-to-signal by a fixed frequency increment Δf . The frequency of the Nth signal can be written as

$$f_i = f_0 + i\Delta f$$

where f_0 is the starting carrier frequency, Δf is the frequency step size, that is, the change in frequency from signal to signal, and $0 \leq i \leq n-1$. Each signal dwells at each frequency long enough to allow the received returns to reach the receiver, such that we have a stationary situation. Groups of *N* signals, also called a *burst*, are transmitted and received before any processing is initiated to realize the high-resolution potential of the waveform. The burst time, that is, the time corresponding to transmission of *N* signals, will be called the coherent processing interval (CPI) [9].

A stepped frequency continuous wave radar determines distance information from the phase shift in a target-reflected signal. Stepped-frequency radar determines the distance to targets by constructing a synthetic range profile in the spatial time domain using the Inverse Fast Fourier Transform. The IFFT method is described in detail by Wehner [5]. The synthetic range profile is a time domain approximation of the frequency response of a combination of the medium through which the electromagnetic radiation propagates, and any targets or dielectric interfaces present in the beamwidth of the radar [5]

If the transmitted signal for the Nth signal is $A_1 cos 2\pi(f_0 + i\Delta f)t$, then the target signal return after the round trip time $(2R/c)$ is $A_2 cos 2\pi(f_0 + i\Delta f)(t - \frac{2R}{c})$. The output of the phase detector can be modelled as the product of the received signal with the reference signal followed by a lowpass filter. This is equivalent to the difference frequency term of the above-mentioned product. For real sampling the phase detector output for the *N*th signal is $Acos\phi_N$, and for the quadrature sampling it is $Ae^{-j\phi_N}$, where

$$\phi_N = 2\pi(f_0 + i\Delta f)\frac{2R}{c} = \frac{4\pi f_0 R}{c} + 2\pi\frac{\Delta f}{T}\frac{2R}{c}iT$$

for a stationary target case. The first term of this equation represents a constant phase shift. The second term represents a shift in frequency during the round trip time. The second term is the multi-

plication of the rate of change of frequency $\frac{\Delta f}{T}$ with the round trip time. The range is converted into a frequency shift f_s . Thus it is possible to resolve and measure the range to the target by resolving the frequency shift in the phase equation. The range to the target can be obtained by rewriting R in terms of f_s as $R = \frac{c}{2}\frac{T}{\Delta f} \times f_s$. The output of the phase detector is quadrature sampled into N complex samples. The DFT of N data samples resolves the range bin into fine range bins of width, $c/2N\Delta f$. DFT coefficients represent the target reflectivity of different parts of a range bin or an extended target within a range bin. Plots of the magnitude of DFT coefficients are often called high resolution range profiles [9].

For a single target at a constant range , R, there will be a linear change in the phase for each frequency step f_i . The real and imaginary parts of the data will therefore be sinusoidal with a frequency corresponding to the phase unwrapping rate. Targets closer and further away are expected to produce respectively lower and higher phase unwrapping rates. The reader is referred to appendix A of this dissertation for a comprehensive treatment of the principle of SFCW radar. Rerefences [5, 6, 7, 2, 9] also cover this principle in detail. Earlier work was done by Fowler et al [10].

2.3 Stepped Frequency Ground Penetrating Radar

Stepped frequency continuous waves used in GPR radars are very powerful. This is because in ground penetrating applications, large bandwidth is required to solving the problem of locating, detection and identifying subsurface features as explained in section 1.1. Figure 2.1 shows a simple block diagram of a stepped frequency ground penetrating radar. In practise a signal generator generates a single frequency pulse and the frequency synthesizer allows the pulse-to-pulse frequency variation. A single frequency is transmitted into the propagation medium at a time . If there is some discontinuity in the dielectric property of the material, a fraction of the transmitted power will be reflected back. In the block diagram, figure 2.1, a simple case of a buried object is shown under a few meters of soil.

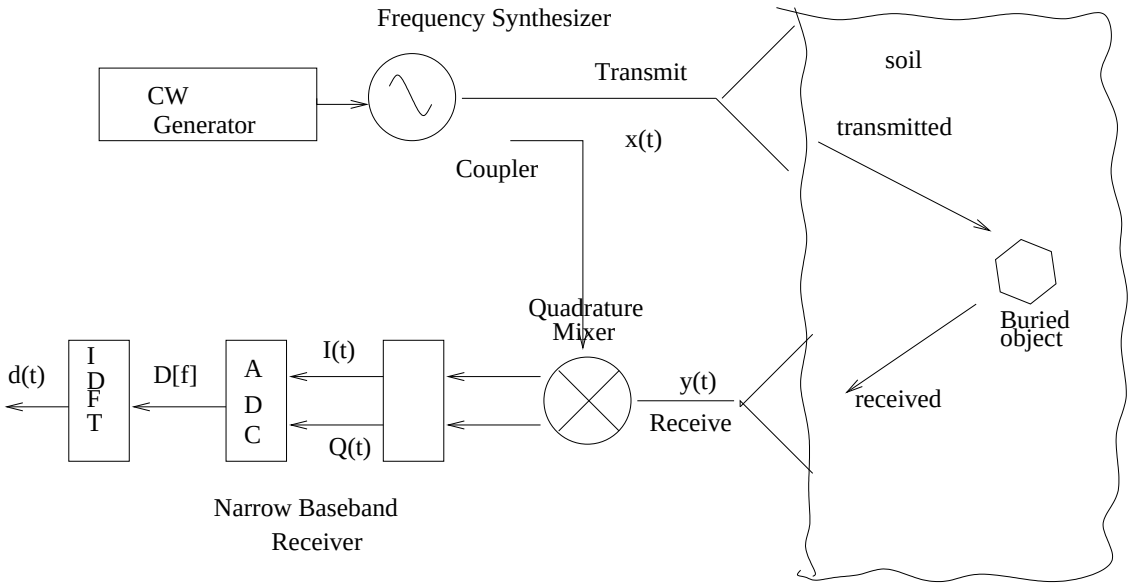

Figure 2.1: A simple block diagram of a SFCW GPR radar, taken from Noon [2], redrawn by the writer using Xfig.

There is a difference in the dielectric property ε_r of soil and the buried object, this difference is what we generally call discontinuity. Therefore, the transmitted signal experiences attenuation when it enters the medium and discontinuity when it propagates from soil to the object. The reflected signal is "picked up" by the receive antenna, and compared to the transmitted signal, both magnitude and phase measurements are taken. The complex frequency information is mapped into the time domain by the Inverse Discrete Fourier Transform (IDFT). The time domain representation is what we call the synthetic range-profile. Reference [9] discusses this theory in detail.

2.4 Modelling Transmitted and Received Signals

The *Helmholtz wave equation,* which can be derived from Maxwell's equations for plane waves propagating through a *general lossy medium* is used and is described by Langman et al [1] and Noon et al [2]. A solution to the Helmholtz wave equation is the electric field $E(z)$, described by the following equation:

$$E(z) = E_o e^{-\gamma z} = E_o e^{-\alpha z} e^{-j\beta z}$$

E_o is an electric field constant, γ is the propagation constant, which is made up of real and imaginary component: attenuation constant α and phase constant β. For different media, the Helmholtz wave equation is exploited as described by Langman [1]. If the transmitted signal is $E_t = E_o e^{-jwt}$, where w is the angular frequency ($w = 2\pi f$, where f is the electromagnetic frequency). Since the interface

has some complex reflection coefficient s. The received signal at a distance R beneath the surface is given by

$$E_r = s\frac{E_t}{d^2}e^{(-2\alpha R)}e^{(jwt-2\beta R)}$$

If more targets are present, the reflections will add up both in magnitude and phase. By stepping through the frequency through *n* steps and taking the Fourier transform, the individual targets can be resolved. According to Kabutz et al [8], it has been shown that the range bin spacing Δz based on the Fourier series is

$$\Delta z = \frac{c}{2n\Delta f\sqrt{\epsilon_r}}$$

where Δf is the frequency step, *n* is the total number of frequency steps, ϵ_r is the relative dielectric constant (or relative permittivity) of the propagation medium, and c is the speed of light. Kabutz [8] further explains that the corresponding unambiguous range of the stepped frequency GPR radar in a lossy medium is thus:

$$R_{unam} = (n-1)\Delta z$$

The range resolution is given by this code computes the average sample value per frequency for the Q channel

%there should be 64 average values since there are 64 frequencies per channel

$$\Delta R = \frac{c}{2B_{tot}\sqrt{\varepsilon_r}}$$

The required bandwidth to achieve this resolution and this unambiguous range is thus:

$$B_{tot} = (n-1)\Delta f$$

The equations described in this section are used to introduce the simulation requirements in terms of the system bandwidth, the frequency step size, the number of frequency steps and the relative permittivity of the medium. The modification of the radar equation to account for the medium characteristics is further discussed in chapter 4.

2.5 Introducing Simulation Specifications

2.5.1 Transmitter Specifications

2.5.1.1 Bandwidth

In stepped-frequency continuous waves, the total radar bandwidth is wide but the instantaneous bandwidth is narrow, since a group of narrow band continuous waves are transmitted. A known relationship between a waveform of width τ and bandwidth is $B = 1/\tau$. Thus for large bandwidths, the pulse width must be small. But to obtain high resolution, wide bandwidth is necessary for SFCW GPR radars. For this simulation, the required transmitter bandwidth is the range 1MHz - 100MHz. In soil with a dielectric constant $\epsilon_r = 6$, this 99MHz bandwidth provides a range resolution given by:

$$\Delta R = \frac{c}{2B_{tot}\sqrt{\varepsilon_r}} = \frac{2.998 \times 10^8}{2 \times 99 \times 10^6 \times \sqrt{6}} = 618.15mm$$

This is high range resolution. The above-used permittivity constant value for the medium (soil) was taken from the terms of reference. The simulation can be easily adaptable to a wide range of soil types and resolution requirements, simply by solving for the range resolution above and adjusting the losses in the simulation appropriately. That is, for a certain resolution between targets buried in a medium with a known permittivity, the bandwidth can be computed by rearranging the equation. Then the simulation will be properly adjusted.

2.5.1.2 Frequency Stepsize

The frequency stepsize, Δf , is the amount by which the frequency changes from signal to signal. Frequency stepsize is given by

$$\Delta f = B_{tot}/(n-1) = \frac{99 \times 10^6}{(32-1)} = 3.2MHz$$

for n = 32, where n is the number of frequency steps taken. The unambiguous range of the SFGPR radar depends on the number of steps taken and the bandwidth used. Since a Discrete Fourier transform is used on the received data only powers of 2 are taken, that is, $n = 2^x$. For this simulation the writer used $n = 2^5 = 32$. The theoretical unambiguous range required for this specific application can be found by calculating at what range the return form a particular target in the lossy medium will no longer be visible. The theoretical unambiguous range is obtained to be:

$$R_{unam} = \frac{c}{2B_{tot}\sqrt{\epsilon_r}}(n-1) = \frac{2.998 \times 10^8}{2 \times 99 \times 10^6\sqrt{6}}(32-1) = 19.163m$$

For purposes of the simulation and for most GPR applications, a theoretical unambiguous range of this magnitude ($\simeq$19 m) is sufficient. Also this is the range where we begin to be unable to differentiate between two targets separated by a small distance which is satisfactory for a GPR.

2.5.1.3 Transmitter Power

The transmitted power, P_t , from a transmitting antenna is required to be 10 dBm. The gain of the antenna G_t equals 0 dB and the temperature of the antenna can be taken as room temperature $T_a = T_0 = 290K$, in Kelvin.

2.5.2 Propagation Medium Specifications

A propagation medium has an electric permittivity ε and conductivity σ . A plane wave propagating in the z direction into the medium can be described by the Helmholtz wave equation shown in section 2.4. The attenuation constant in the Helmholtz equation α is expressed in Nepers per metre [Np/m]. However the ground material attenuation is expressed in decibels per metre [dB/m], $\alpha[dB/m] = 8.686\alpha[Np/m]$. Most media are low loss non-magnetic (that is $\mu = \mu_0$) media, and approximations of the attenuation constant and phase constant for such media are:

$$\alpha = \frac{188.5\sigma}{\sqrt{\varepsilon_r}}$$

and

$$\beta = \omega\sqrt{\mu\varepsilon_r}$$

where $\varepsilon_r = \varepsilon/\varepsilon_0$, the relative permittivity or the dielectric constant of the medium. The phase constant β can be converted to a phase velocity $\nu = c/\sqrt{\varepsilon_r}$. It has been shown, [2] , that a constant ε_r across a frequency range results in a constant phase velocity and a linear relationship in the attenuation versus frequency graph. For a permittivity $\varepsilon_r = 6$, the phase velocity is $\nu = 1.2239m/s$ and the attenuation constant is $\alpha = 76.955\sigma$. This attenuation, caused by the ground, modifies the radar equation by $e^{-4\alpha R}$ such that the received power, assuming the far filed pattern antenna, P_r , is then given by

$$P_r = \frac{P_t G_t G_r \lambda^2 \sigma_t e^{-4\alpha R}}{(4\pi)^3 R^4 L_s}[W]$$

where σ_t is the radar cross section of the target, λ the wavelength in the ground, L_s accounts for all the losses in the system and R is the range to the target. The radar cross section in this case can be calculated from the permittivity change between the surrounding medium and the target as shown by Noon [2] .

However for our simulation purposes and for comparison to impulse GPR purposes, the main requirement of the propagation medium is that it should attenuate the signal with an attenuative loss of 10 dB. Furthermore as already mentioned above the permittivity of the medium can be assumed as a constant value $\varepsilon_r = 6$.

2.5.3 Receiver Requirements

2.5.3.1 Bandwidth

The entire transmitted frequency range must b*e* recovered by the RF stage of the receiver. The RF stage is where the frequency of the received waveform is still equal to the frequency of the transmitted waveform. Too much *gain* in the RF stage of the receiver can easily cause *saturation* in the receiver and eventually a loss in the dynamic range. **Gain** can be simply described as the amount of signal amplification in the receiver architecture and **saturation** is simply a term used when a device has reached the point where the output signal cannot go up in magnitude irrespective of the input. The gain of the system must be evenly distributed throughout the RF and IF stages of the receiver. The Intermediate Frequency stage is the frequency stage between baseband and RF frequency stage.

2.5.3.2 Dynamic Range

It is a known fact that non-linear devices such as amplifiers generate spurious frequency components at very high frequencies. In either case, these effects set a minimum and maximum realistic power range over which a given component or network will operate as desired. This power range is termed the *Dynamic Range* . Dynamic range can be divided into *linear Dynamic range* and *spurious-free Dynamic range.*

The *linear* dynamic range is limited by noise at low end and by the 1dB compression point at high end, that is , $DR_l = P_1 - N_o$. The *spurious-free* Dynamic range is the range where spurious responses are minimal, it is limited by the noise at low end and by maximum power level for which intermodulation distortion becomes unaccepatble $DR_f = \frac{2}{3}(P_3 - N_o - SNR)$. The reader is referred to Appendix A of this dissertation for a well summarised description of the Dynamic range. The design of the simulation was made to attempt to achieve a dynamic range according to the ADC specifications as follows.

2.5.3.3 Analogue to Digital Conversion

According to Farquharson et al [11] , the receiver dynamic range specifies the number of bits required by the radar sampling system. A 12 bit analogue to digital converter can achieve a theoretical 65 dB

signal to noise ratio (SNR), a 14 bit 77 dB SNR and a 16 bit 89 dB SNR. If the receiver dynamic range is greater than that of the ADC, then the required dynamic range will determine the requirements of the analogue to digital converter. The user requested a 14 bit ADC or quantiser, this ADC will yield a theoretical 77 dB dynamic range of the receiver. Therefore the dynamic range of the simulation was made to attempt to achieve this theoretical value. The sampling frequency for the ADC is one mega samples per second (1MS/s) and 128 samples per frequency must be taken.

2.5.3.4 Typical Receiver Requirements

Furthermore, Pozer et al [12] reckons a well-designed receiver must provide the following requirements:

- *High gain* ($\sim$100 dB) to restore the low power of the received signal to a level near its original baseband value
- *Selectivity*, in order to receive the desired signal while rejecting adjacent channels, image frequencies and interferences
- *Down-conversion* from the received RF frequency to an IF frequency for processing
- *Detection* of the received analog or digital information
- *Isolation* from the transmitter to avoid saturation of the receiver.

The simulation bears the above-stated requirements. The writer explains in subsequent chapters the methods used to meet these requirements and give reason where these requirements were not met. The next section summarises the simulation design requirements in table form.

2.6 Summary of Simulation Requirements

The following table summarises the above requirements that the simulation must meet:

Parameter	Symbol	Formula	Value
start frequency	f_0		1MHz
stop frequency	f_U		100.2MHz
total bandwidth	B_{tot}	$f_U - f_0$	99MHz
number of frequency steps	n		32
frequency step size	Δf	$B_{tot}/(n-1)$	3.2MHz
coherent processing interval	CPI		32ms
dwell time per frequency	T_{dwell}	CPI/n	1ms
range resolution	ΔR	$\frac{c}{2B_{tot}\sqrt{\varepsilon_r}}$	618.15mm
maximum unambiguous range	R_{unam}	$\frac{c}{2B_{tot}\sqrt{\varepsilon_r}}(n-1)$	19.163m
time resolution (two way)	Δt	$1/B_{tot}$	10.10 ns
relative permittivity of medium	ε_r		6
Transmitter Power	P_t		10mW
Analogue to Digital converter	ADC		14bit
Dynamic Range	DR	$\frac{2}{3}(P_3 - N_0 - SNR)$	> 77dB

Table 2.1: Summary of the 32 frequency step SFGPR simulation requirements.

These above mentioned requirements set a standard for our radar simulation. The calculated values are used as basis for simulating both the transmitter and the receiver architecture. The next section briefly explains the important distinction between a SFCW radar and FMCW radar system.

2.7 Distinction between SFCW and FMCW

The ability of the FMCW radar to sweep across wide frequency bands and obtains high resolution is attractive to GPR. However, due to its continuous nature, FMCW radar has a major limitation of a reduced receiver dynamic range. The IDFT is used to transform the different beat frequencies of the targets to a time profile where the travel times to the targets are well resolved according to the FMCW bandwidth. The FMCW radar instantaneously transmits and receives signals using two antennas. The range sidelobes of the leakage signal between the two antennas can " mask" the smaller signals reflected from deeper targets. Because of the continuous nature of the waveform it is not possible to use sensitivity time control commonly used in impulse radars. Methods have been investigated two cancel the leakage signal in the FMCW receiver [13], however to the author's knowledge the techniques does not offer a practical solution for GPR, where the leakage signal can change dramatically in amplitude and phase with small variations in surface roughness.

Stepped-frequency radars are quite often confused with FMCW or swept-FM radars because of their linear frequency transmission, down-conversion in the receiver and the IDFT performed on the sampled data. There is, however, a technical distinction between these radar types. FMCW measure the travel time of a signal directly from the difference in frequency (that is, the beat frequency,

$f_b = Bt_t/t_d$, where t_t is the travel time of the signal and T_{dwell} is the dwell time) between the receiver and reference paths. The IDFT is used to transform the different beat frequencies of the targets to a time profile where the travel times to the targets are well resolved according to the FMCW bandwidth. FMCW do not require the in-phase and quadrature components of the received signals to reconstruct the time profile Taylor et al [9].

On the other hand, the stepped-frequency radar measures the travel time of the reflected signals by measuring the phase difference between the receiver and reference paths at each frequency. In-phase and quadrature samples must be taken at each frequency step to measure the phase. An IDFT is then used as a matched-filter, to properly construct the synthesised time profile [5]. This discrete distinction is an extract from David Noon's PhD thesis [2] section 1.2.1.

2.8 Summary

Concepts developed in this chapter can be summarised as follows. A stepped frequency waveform can be realised by linearly incrementing the frequency of each of the *n* pulses by a fixed frequency stepsize Δf. The resultant stepped frequency waveform will have a bandwidth $B = \Delta f(n-1)$. The return from a target at distance R from the radar will be shifted in phase. A SFCW radar then determines distance information from the phase shift in a target-reflected signal. The output of the phase detector is

$$\phi_N = \frac{4\pi f_0 R}{c} + 2\pi \frac{\Delta f}{T}\frac{2R}{c} iT$$

The second term, $\frac{\Delta f}{T}\frac{2R}{c}$, represents a shift in frequency during the round trip time. The range (or distance) R is converted in the frequency shift f_s . The range to the target can be obtained by rewriting R in terms of f_s as $R = \frac{c}{2}\frac{T}{\Delta f} \times f_s$. The output of the phase detector is quadrature sampled into N complex samples. The DFT of N data samples resolves the range bin into fine range bins of width, Δz . Plots of the magnitude of DFT coefficients are often called high resolution range profiles. When the stepped frequency waveforms described above are used in ground penetrating radars, the range bin spacing equation, the unambiguous range and the range resolution are modified as shown in section 2.4. The modified equations take into account the ground characteristics. The simulation specifications are well summarised in table 2.1, where for *n* equals 32 the theoretical unambiguous range is 19.163 m, for a constant relative permittivity of the ground of $\varepsilon_r = 6$. The terms of reference specifies an analogue to digital converter using 14 bit, which means the theoretical dynamic range must be greater than 77 dB [11]. For completeness, Noon's differentiation of SFCW and FMCW is included [2] . The main difference between the two is, FMCW measure the travel time of a signal directly from the difference in frequency (that is, the beat frequency, $f_b = Bt_t/t_d$, where t_t is the travel time of the signal and t_d is the dwell time) between the receiver and reference paths. On the other hand, the SFCW measures the travel time of the reflected signals by measuring the

phase difference between the receiver and reference paths at each frequency. In-phase and quadrature samples must be taken at each frequency step to measure the phase. The following chapters introduce the simulation design using the above calculated parameters. We firstly start the simulation design with transmitter simulation discussed in chapter 3.

Chapter 3

The Transmitter

3.1 Introduction

The transmitter is the heart of a continuous wave system, since the coherency of the transmit-receive signals determines the accuracy of the measurements [8] . This chapter discusses the simulation design of the transmitter of a stepped frequency ground penetrating radar and its performance. It was noted that there are numerous ways of simulating a stepped frequency radar transmitter in SystemView. Two of these methods are mentioned in passing in this chapter, however emphasis is given to the simulation that was chosen for this project . The reader must note that the design used for the transmitter is not similar to the one described in most textbooks [5, 6, 7, 9], but rather serves the purpose. In SystemView there are ways in which most of the practical design requirements (for instance, the actual frequency synthesizer block in the transmitter) can be eliminated without losing the essence of the simulation. In the simulation of the transmitter, the main interest lies in the output of the transmitter.

3.2 Frequency Synthesizer Design

In practise a frequency synthesizer is the ideal Stepped Frequency Continuous Wave transmitter in terms of frequency stability and reproducibility [5, 8, 9] . The frequency can be made highly stable and accurate at the cost of increasing complexity. This design has been widely used in stepped frequency radar and is very successful. However simulating a frequency synthesizer can be time consuming for this project, therefore alternatives have been investigated. For reasons mentioned above, a less time consuming simulation was used and the synthesizer is mentioned here for completeness.

3.3 Various Transmitter Simulation Designs

There are various ways one can simulate a stepped frequency radar transmitter in SystemView. These methods are briefly described below and depending on the reader's knowledge of SytemView, improvements can be made. The project supervisor, Professor Michael Inggs, suggested these different configurations of the transmitter design, except where stated.

3.3.1 Staircase waveform mixed with a Voltage Controlled Oscillator

- By creating a staircase waveform with the number a steps equal to the number of frequency steps. Then driving the input of a Voltage Controlled Oscillator with the staircase, a stepped frequency continuous wave can be realised. The staircase waveform can be produced by combining a number of step functions shifted in time. An Alternative to producing a staircase will be to use the custom token from the Function library and define an algebraic equation for the staircase of interest. A Voltage Controlled Oscillator can simply be realised by appropriately defining the Frequency Modulation (Fm) token of SystemView, this operation is briefly described by the help document of SystemView.

Disadvantages of this configuration

There are three major disadvantages of this configuration. First, to generate the staircase, either *n* step functions need to be combined to obtain *n* steps in the staircase, or some complex algebra has to be integrated to achieve the desired number of steps in the staircase if the custom token is used. Secondly, the start and stop time, that is, the dwell time, for each frequency is difficult to set accurately. Thirdly, voltage controlled oscillators normally produce lots of harmonics which can result in the drift of the carrier frequency. Suppression of the frequency drift, will require extra time for the phase-locked loop design. Phase-locked loop systems are available in SystemView but their analysis needs careful thinking.

3.3.2 Matlab in SystemView

- The second configuration will be to write a Matlab code that produces the stepped frequency continuous wave and use the code as an input to a SystemView system. Incorporating Matlab into SystemView is found in the C++ link in SystemView. This configuration was suggested by Guma Kahimbaara, a member of RRSG.

Disadvantages of this configuration

With Matlab being another complex programming language, for non-programmers or design engineers not familiar with Matlab, creating a Matlab code that simulates a stepped frequency is difficult. This is one major drawback of this configuration. However for design engineers familiar with Matlab, this operation can be fairly easy and this configuration can be a good option. However, linking Matlab into SystemView can be a thought provoking process.

Advantages of this configuration

If the code for a stepped frequency waveform is correctly synthesised, a powerful stepped frequency generator can be realised. This is because, the Matlab code can be accurately programmed without any frequency errors, such that the stepped frequency signal has a specific unchanging start time and stop time. The frequency transition at the end of each dwell time can be made extremely smooth and accurate, avoiding errors associated with frequency inaccuracy.

Other methods are also available, but those are left out in this thesis. The writer now describes the configuration used to simulate the stepped frequency continuous waveforms and eventually the transmitter.

3.4 Stepped Frequency Continuous Wave Generation

Since this project has time constraints, the disadvantages associated with the above-mentioned methods cannot be tolerated. They can waste a lot of time and therefore not desirable in this project. The transmitter simulation used is discussed in this section. The simulation of the transmitter is divided into two parts. The first part discussed is the generation of the stepped frequency waveform. The second part is the transmit antenna.

A far less time consuming configuration, was the use of the Variable Parameter Editing token found under Tokens in the SytemView horizontal toolbar. By specifying the number of system loops in the variable parameter specification window and the variable whose value had to be change after every system loop (in this case, frequency), a desired stepped frequency signal was obtained.

Simple SystemView Method of Stepped Frequency Simulation

To generate a stepped frequency wave simulation with: $f_0 = 1MHz$ $f_U = 100.2MHz$ $\Delta f = 3.2MHz$ and n = 32 frequency steps. The writer started with a sinusoid at 1 MHz and 10 mV, from the Source token. In the system window under Tokens, the New Variable Token option was selected.

A New Variable Token Specification window appeared, in this window the frequency of the sinusoid was selected as a parameter whose value was going to be variable during the simulation execution. SystemView calls the number of frequency steps, the number of loops. Thus 32 was used for the number of loops. The frequency step size value, Δf was specified under Auto Increment Parameters. Clicking on increment automatically stepped the frequency by the specified ,Δf , value from signal to signal. The increment button also automatically set the amplitude of all signals at the same value of 10 mV. However the order is important, number of loops first, the frequency increment value, then increment.

To control how long each signal was transmitted before moving on to another frequency, that is, the dwell time, the writer used the system time window. The dwell must be equal to the stop time. To avoid the dwell time from changing, the start and stop time were locked. If the start and stop times are not locked, then changing either the system sample rate or the number of samples will change the start and stop time as well. If the maximum frequency in the simulation is *f* , then make the sample rate four *times f* , this is a special requirement by SystemView. For this simulation the system sample rate was 400MHz. The above-described SV operation completed the desired stepped frequency continuous wave generator.

A note on the stop time

For this simulation, each frequency in the waveform was transmitted for T = 1ms allowing at least a thousand cycles of each frequency to be transmitted before stepping into another frequency. It was important to specify a stop time larger than $1/f_i$, for each f_i transmitted, to ensure that the entire signal bandwith was transmitted. For instance, for this simulation $f_0 = 1MHz$ implying that $T_0 = 1000ns$, therefore the stop time must be more than a thousand nanoseconds to be able to transmit the entire f_0 signal. A dwell time equals one millisecond is sufficient to allow also the transmitted signal to be received before moving on to the next frequency. This dwell time yields a total transmitting time (or CPI) of 32 ms. To avoid using the output of the previous loop (or frequency step) as the input to the next loop, the Reset System on loop condition was set in the system time window. It was noted that the number of loops in the system time window, was already changed to 32. This was because the number of loops was already specified in the New Variable Token Specification window. Again the order is important.

Advantages of this Configuration

The following are the advantages of using this configuration to simulate a stepped frequency continuous waveform in SystemView:

1. To the writer's knowledge, this is the most simple and less demanding method of generating the SFCW waveform in SystemView.

2. The technical facts involved in generating a SFCW are eliminated without any loss in the integrity of the output signal. The technical facts might be, simulating frequency synthesisers, or voltage controlled oscillators which is eliminated by this methodology.

3. The simulation is highly adaptable, that is, the number of frequency steps can be easily changed by simply changing the number of system loops. This is the major advantage of using this method compared to others. Also, the frequency stepsize can be easily changed by redefining the increment value in the variable parameter token

3.5 Transmit Antenna Simulation

The simulation of the transmit antenna was kept simple. From the theory of antennas it is known that antennas would provide a gain G_a of certain magnitude to the transmitted signal. The gain of an antenna is given by $G_a = A_e \frac{4\pi}{\lambda^2}$. A_e is the effective aperture area of an antenna, related to the directivity of the antenna, and λ is the operating wavelength of the antenna. Most antennas behave differently, but there is one common factor in them. They all provide a certain gain to the signal and to the writer knowledge, almost all the time introduce noise into the signal.

For the simulation of the transmit antenna, a filter model was used to simulate the behavior of an antenna at the frequency range of interest. The gain of the antenna was made 0 dB for the frequency range of 1-100.2 MHz. A three-pole Butterworth Lowpass Infinite Impulse Response (IIR) filter with a cutoff frequency of 100.2 MHz was designed. The gain versus frequency plot of this filter design shows a constant gain of 0dB from 0-100 MHz. The noise that the antenna introduces was simulated thermal noise at 300 K added to the signal. Not all antennas, simply just amplify the signal, signal attenuation in some of the antennas takes place. The reader is referred to [12] chapter 4, page 131, about practical antennas. The RF and Analog library attenuator was used to simulate the attenuation introduced by some antennas. The block diagram showing how the noise, the attenuator and the filter model are connected in the system is shown in figure 3.1 . The SystemView diagram of the simulated antenna can be found in Appendix B.

3.6 Transmitter Performance

The performance of the transmitter was analysed by viewing the frequency spectrum of the transmitted signals from the antenna. This was done by sweeping the transmitter over the entire frequency range, and observing the power spectrum of the transmitted signals. It is known from theory that, the

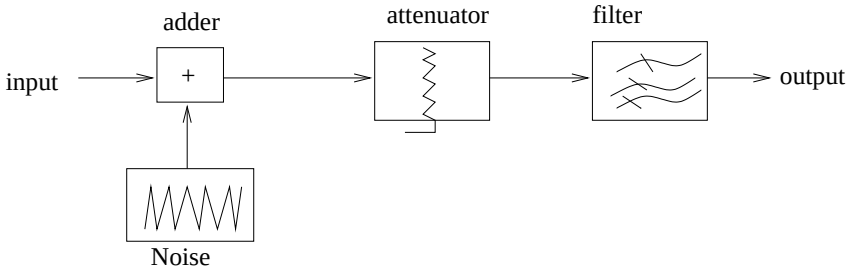

Figure 3.1: Block diagram of an antenna showing how different tokens are connected.

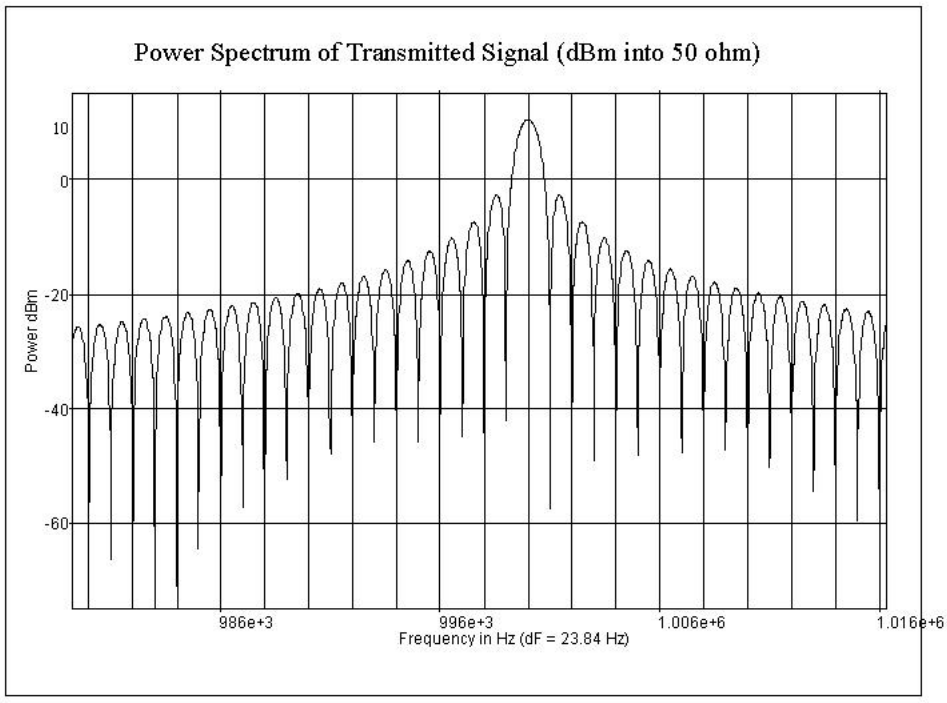

Figure 3.2: Power spectrum for the transmitted signal at 1 MHz.

power spectrum of stepped frequency waveforms in the frequency domain looks like a train of spikes (or dirac deltas). Each spike in the train is located at every signal frequency, that is $f_i = f_0 + i\Delta f$. This fundamental theory was used to test the performance of the transmitter. Shown in figure 3.2 , is the spectrum for one transmitted signal at 1 MHz.

The observed spike for the power spectrum is located at 1MHz. The difference between the location of the spikes is $\Delta f = 3.2MHz$. The power spectrum plot indicates an average 10 dBm value of the transmitted power, which is equal to the 10 mW. Furthermore, not all the signals have the same transmitter power of 10 dBm, but this cannot be regarded as frequency drift. Therefore, the generated SF wave has no frequency drift, even though some signals do not exactly have a power level at 10 dBm.

3.6.1 Spectral Purity

The enlarged version of the power spectrum of the transmitted stepped frequency waveform is shown in the figure 3.2 . It serves to show the purity of the spectrum. Each transmitted signal stands out from the noise and peaks at the carrier frequency. It is apparent from this figure that the transmitted waveform has a power level of 10 dBm at 1MHz and at most frequencies. Some frequencies are in the 10 dBm vicinity throughout the entire bandwidth of 99 MHz.

The signal to noise of the stepped frequency is the best way of testing for the purity of the signal. The statistics button in the Analysis Window of SystemView provides useful information about the windows open in the Analysis Window. It provides the mean value of the noise in dBm and the minimum and maximum value of the signal in dBm. By taking a difference between the signal and the noise, we obtain the signal to noise ratio of the stepped frequency waveform. For the transmitted stepped frequency waveform, the maximum signal value, after the transmit antenna described in section 3.5, is $S = 10dBm$. The mean value of noise is $N = -79.3dBm$. This gives a signal to noise ratio of $S/N = 89.3dB$. This is a good signal to noise ratio at the transmit side of a radar system.

3.6.2 Phase Noise

The time domain plot of the transmitted stepped frequency waveform depicts little unwanted spikes (pointed with an arrow in figure 3.3) which represent the sudden frequency changes at the end of each dwell time. This sudden change in the frequency results in the sudden change in the phase, which causes phase noise. Figure 3.3 depict the continuous waveform at the end of the first transmitted signal and beginning of the second signal.

3.6.3 Frequency jitter

Kabutz [8] , defines frequency jitter as any unwanted phenomena that was observed on the transmit frequency. To have a clear vision of the frequency jitter, it was required that the power spectrum of one signal be taken, enlarged and observed over the dwell time 3.2. Even though it does not satisfy the definition of frequency jitter, it was observed that not all signals have power levels at 10 dBm. This was regarded as the only frequency jitter. The little spikes at the end of each dwell time caused phase noise. This is however not frequency jitter see figure 3.3.

3.6.4 Range-Profile Distortion Produced By Frequency Error

It is important that frequency accuracy be achieved. According to Wehner et al [5] , any frequency deviation from $f_i = f_o + i\Delta f$ results in distortion of the synthetic range profile. However, a constant

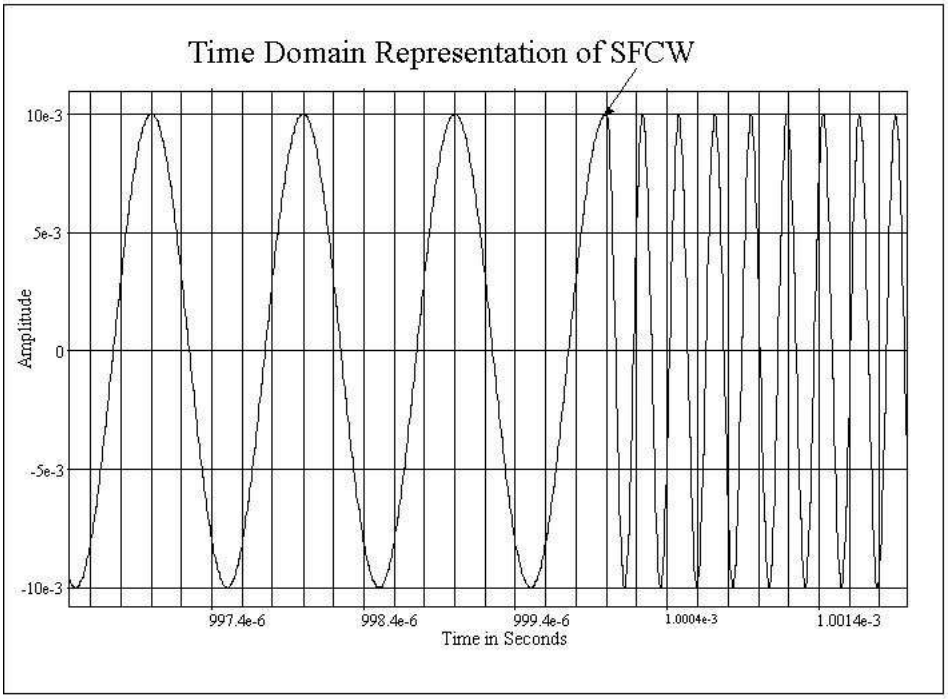

Figure 3.3: Time Domain Representation of the transmitted SFCW waveform

error in the frequency over the measurement bandwidth does not degrade the range resolution and the unambiguous range since these two quantities do not depend on the actual frequency (*see their respective equations above)* but rather on the total radar bandwidth. An error in Δf will cause a limit in the dynamic range of the synthetic range profile after Fast Fourier Transform (FFT) processing. This is because the magnitude of the synthetic range profile at range R and zero target velocity is defined by

$$|H_i| = \left| \frac{sin(\pi y)}{n.sin(\pi y/n)} \right|$$

where $y = \frac{-2nR\Delta f}{c} + i$ and a positive interger i is $0 \leq i \leq n-1$. Wehner et al [5] , further explains how to ensure frequency accuracy using a standard deviation technique, however this is not necessary in this simulation since SytemView ensures frequency accuracy by allowing the user to preset the desired frequency values before running the simulation. These frequency values are not changing during the simulation as shown by the plots above.

3.7 Summary

The simulation of the transmitter can be summarised as follows. A stepped frequency continuous wave transmitter was simulated. It has a start and stop frequency of 1 MHz and 100 MHz respectively.

Each frequency is transmitted for a millisecond, this is what we call the dwell time per frequency. The number of frequency steps taken is *n* equal to 32 for a frequency stepsize of 3.2 MHz. Both the number of frequency steps taken and the frequency stepsize are easily adaptable in SystemView. This means to change the number of steps and the stepsize simply requires retyping the correct values in SystemView. This is one major advantage of using the Token Parameter Variation method, instead of using the two methods described in subsection 3.3.1 and 3.3.2. The maximum transmitted frequency sets the system sample rate to 400 MHz, this is a special SystemView requirement. The performance of the transmitter was evaluated by viewing the spectrum of the transmitted waveform. As required by the specifications of the transmitter simulation, the transmitter power was 10 dBm, which is equivalent to 10 mW. The spectral purity of the transmitter was justified by the signal to noise ratio of 110 dB at the output of the transmitter. Phase noise was observed at the point where each frequency changes. Even though it does not satisfy the definition of frequency jitter, it was observed that not all signals have power levels at 10 dBm. This was regarded as the only frequency jitter. The little spikes at the end of each dwell time caused phase noise. This is however not frequency jitter see figure 3.3. The accuracy of the transmitted frequencies was also observed from the spectrum plots and each signal was seen to be located at its transmit frequency.

Chapter 4

The Propagation Medium

4.1 Introduction

The propagation of electromagnetic energy is the key physical phenomenon that makes wireless communication possible [12] . The medium in which these electromagnetic waves propagate is investigated in this chapter. The writer characterise the propagation medium into a simple model. The word medium in this report will mean the propagation medium. The simulation of both the simple model and the real ground characteristics of the medium are discussed. Since a GPR system simulation is being described in this report, the medium is the subsurface, to be more exact, simple ground soil.

GPR radars operate by transmitting electromagnetic waves into the ground, to obtain information about the subsurface features. According to Noon [2] , GPR performance is expressed in terms of two interdependent characteristics: *maximum penetration depth* and *depth resolution*. For GPR, maximum penetration depth relates to the maximum depth at which a buried target can be detected, and the depth resolution is the minimum separation in depth between two buried targets that can be detected. The penetration depth is difficult to calculate as it is a complex function of the ground characteristics [2]. However estimates can be made from simple ground models, this chapter discusses the simulation of these simple ground models.

4.2 Background

GPR is a geophysical method that has been developed over the past thirty years for shallow, high-resolution, subsurface investigations of the earth. GPR uses electromagnetic waves (generally 10MHz to 1000MHz in practise) to acquire subsurface information [14]. Electromagnetic waves are radiated from a transmitting antenna and travel through the material at a velocity determined by the electrical properties of the material. As the wave spreads out and travels downward, if it hits a buried object

or boundary with different electrical properties, then part of the wave energy is reflected or scattered back to the surface, while part of it continues to travel downward as shown in figure 4.1 . These electrical contrasts results in losses of the signal strength, the medium that causes these losses is simulated below.

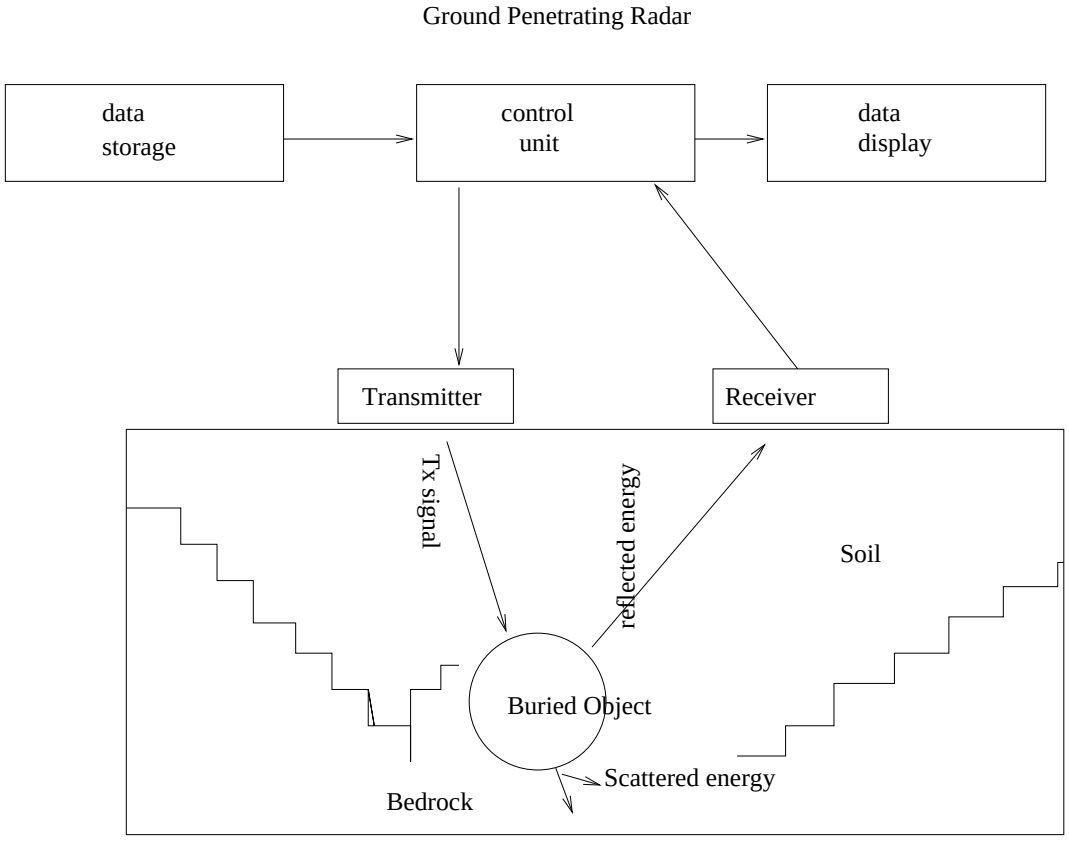

Figure 4.1: Schematic diagram of GPR System

4.3 Simulation of the Propagation Medium

There are two simulations for the propagation medium that were developed. The first simulation was a straight attenuative medium with a loss of 10 dB and a time delay τ . The second medium was the frequency dependent medium, which is the real medium of a GPR, simplified. The second simulation is only discussed in this report, no test are conducted. This simulation attempts to simulate the real behavior of ground characteristics. The two media are described below. Both ideas of the medium come form the writer.

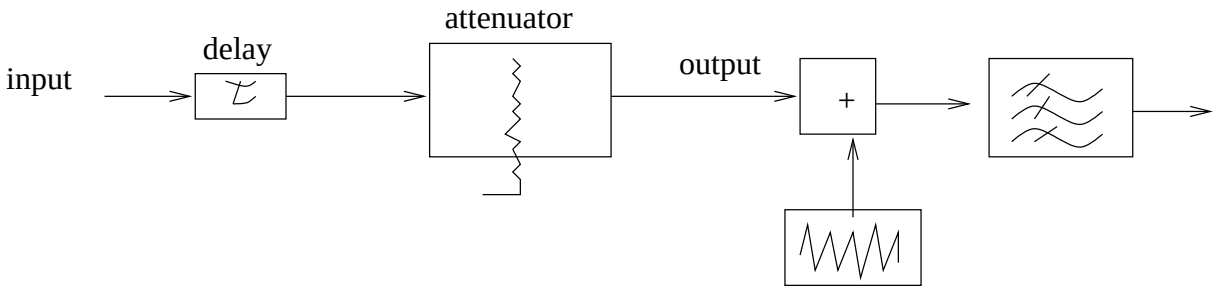

Figure 4.2: The block diagram of an attenuator

4.3.1 Simple Attenuative Medium

When a signal enters the medium, it gets attenuated as explained above. This medium bears only this fact in mind about the medium. In SystemView the received signal was delayed by $312.5\mu s$. The signal was then attenuated by an attenuator from the RF/Analog library of SystemView. The attenuator was set to have the desired value of 10dB. Thermal noise which accounts for the noise that is picked up the signal as it propagates to and from the target was also added. The default value of 300K for the noise was taken for this token as its noise figure is defined by the noise temperature that is close to room temperature. The block diagram of figure 4.2 shows how the tokens of SystemView are interconnected. The SytemView diagram is included in the Appendix B figure B.2.

4.3.2 Frequency Dependent Medium

The frequency dependent simulation of the medium attempts to simulate the behavior of ground characteristics. In the simulation of this medium the following assumptions were made. Electromagnetic waves travel at a specific velocity determined primarily by the electrical *permittivity* ε , of the material. Permittivity is the property that describes the ability of a material to store electric energy by separating opposite polarity charges in space. Relative dielectric permittivity ε_r (previuously called dielectric constant) is the ratio of the permittivity of a material to that of free space. This quantity is of great importance in ground penetrating radars. Consider a plane wave propagating through a linear homogeneous and non-dispersive medium which can be characterised by its complex permittivity ε_r and its complex conductivity σ . The attenuation caused by the ground modifies the radar equation by $e^{-4\alpha R}$ such that the received power, assuming the far filed pattern antenna, P_r , is then given by

$$P_r = \frac{P_t G_t G_r \lambda^2 \sigma_t e^{-4\alpha R}}{(4\pi)^3 R^4 L_s}[W]$$

where $\alpha = \frac{188.5\sigma}{\sqrt{\varepsilon_r}}$ is the attenuation constant of the propagation medium. The permittivity constant for the medium of our choice was 6. Therefore, the attenuation constant is $\alpha = 76.955\sigma$. It is therefore obvious that the attenuation of a medium increases with its conductivity. In general soil

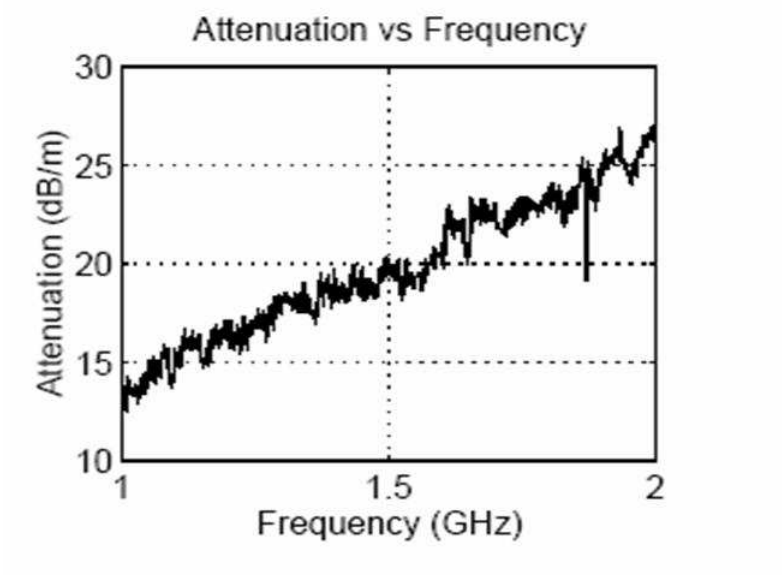

Figure 4.3: Attenuation versus frequency plot showing the linear relationship.

permittivity vary with frequency. Noon et al [2] , page 32 , has shown that a constant permittivity across a frequency range in the GHz region results in a linear relationship in the attenuation versus frequency graph. This fact was used to simulate a model for the medium such that for the frequency range of this simulation, there is a linear relationship between the attenuation and the frequency. The attenuation versus frequency plot taken from Noon [2] is shown in figure 4.3.

In SystemView, from the Operator library a linear system filter can be designed. This can be done by designing a custom FIR filter from the filter design choice. The points of the design can be approximated with the attenuation versus frequency plot shown in figure4.3.

To implement the design the following can be done in SystemView. Starting from the operator library, then chose the linear system filters. The linear filter system window has choices of the type of filter one wants to design, chose the custom filter. Remember that SystemView is designing a filter but this filter is the ground characteristics simulation. Entering the attenuation values for the y-axis and the frequency for the x-axis completes the design of the behavior of the medium.

4.4 Performance of the Propagation Medium

The performance of the simple delaying and attenuating medium is conducted in chapter 6. The effects of the medium are shown at the output of the receive antenna as the received signal. The performance of the frequency dependent medium is shown below.

4.4.1 Frequency Dependent Medium

Since this method was not required for this project, performance testing was not done. This simulation is mentioned as a recommendation for the real ground characteristics.

4.5 Summary

This chapter can be summarised as follows. From the theory on ground penetrating radar systems, it is generally difficult to calculate the penetration depth as it is a complex function of the ground characteristics. Therefore, two propagation medium simulations were made, depicting both the simple ground model and the real ground characteristics. The first medium was a straight attenuative medium with 10 dB loss. The second simulation of the medium attempted to simulate the real behavior of ground characteristics. The second simulation was based on the theory investigated by Noon et al [2] , that there is relationship between the attenuation and the frequency for a constant relative permittivity ε_r . A attenuation versus frequency curve can be simulated using filter models in SystemView to characterise this behaviour of the propagation medium. The performance of the simple medium is shown in chapter 6 and the frequency dependent medium performance is not discussed in this report.

Chapter 5

The Receiver

5.1 Introduction

This chapter introduces the receiver simulation. A well designed receiver will have a high gain to restore the low power of the received signal to a level near its original baseband value. It must also provide selectivity in order to receive the desired signal while rejecting adjacent channels, image frequencies and interferences. Lastly, it must provide isolation from the transmitter to avoid saturation of the receiver [12]. The design of the receiver below strives to meet all these requirements of a well designed receiver.

The chapter starts with a brief summary of receiver architectures that are available to the radar design engineer. The reasons for the preferred architecture for a SFCW radar are explained. Section 5.3 discusses in great detail the simulation of the heterodyne receiver architecture. Each stage of the receiver simulation is discussed independently, and the selection of the components that were used is briefed. The chapter ends with a section that shows the performance of the receiver system. The performance of the receiver system was based on the output SNR, the receiver dynamic range, and the minimum detectable signal (MDS). To avoid intermodulation distortion, a diagram showing the noise and the signal power levels through the stages of the receiver is included. The diagram ensures that P_1 and P_3 are not exceeded.

5.2 Receiver Architectures

There are various receiver architectures that can be designed. The choice of which one to use lies on the particular application and advantages. For a SFCW system, the heterodyne receiver architecture is the best [1]. The homodyne architecture and the heterodyne architecture are briefly discussed below. The advantages of using a heterodyne architecture are the given.

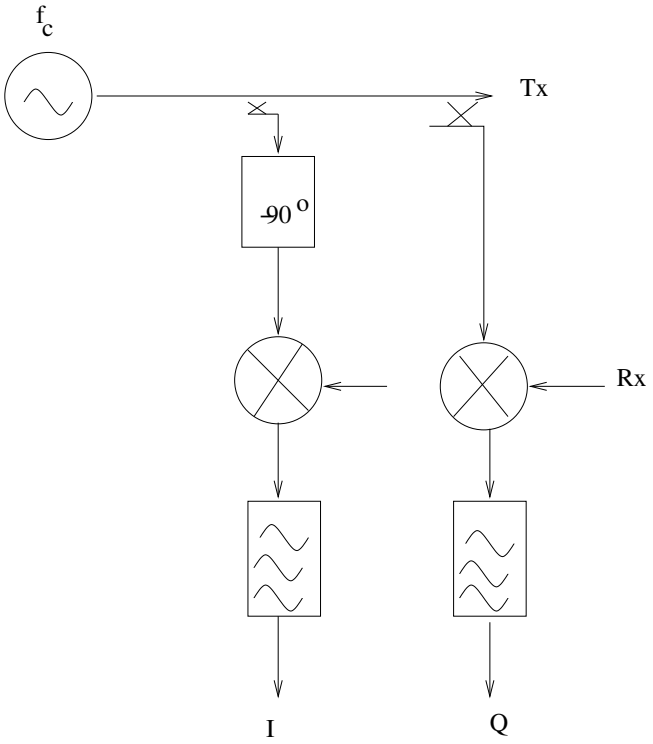

Figure 5.1: Block diagram of a Homodyne Architecture. This figure was taken from [1], and redrawn by the writer using Xfig.

5.2.1 Homodyne Architecture

The homodyne receiver also called the *direct conversion* receiver uses a mixer and local oscillator to perform frequency down-conversion with a zero IF frequency or DC as shown in figure 5.1 below. The local oscillator is set to the same frequency as the transmitted signal, which then converts it directly to baseband. Langman [1] explains that the homodyne has fundamental limitations which limit its use in the development of low cost and high performance SFCW GPR's. These limitations include:

1. The filtering of the RF harmonics across a wide transmit bandwidth
2. The demodulation of the received signals to extract the amplitude and phase information

These problems cannot be neglected and are difficult to solve effectively. This being the reason for the heterodyne system preference.

5.2.2 Heterodyne Architecture

By far the most popular type of receiver today is the *super heterodyne receiver* shown in figure 5.2. A heterodyne radar architecture synchronously detects the radar returns by mixing the received

signal down to an intermediate frequency (IF), and in so doing overcome all of the limitation of the homodyne system. Practically this radar architecture reduces filtering of the harmonics at the RF to a simpler problem of filtering the harmonics at IF. Extracting the I and Q values from the IF can be achieved digitally, by direct IF sampling and quadrature demodulation. The reader is referred to Langman et al [1] ,(pg 137-141), for more details on the homodyne and heterodyne architectures.

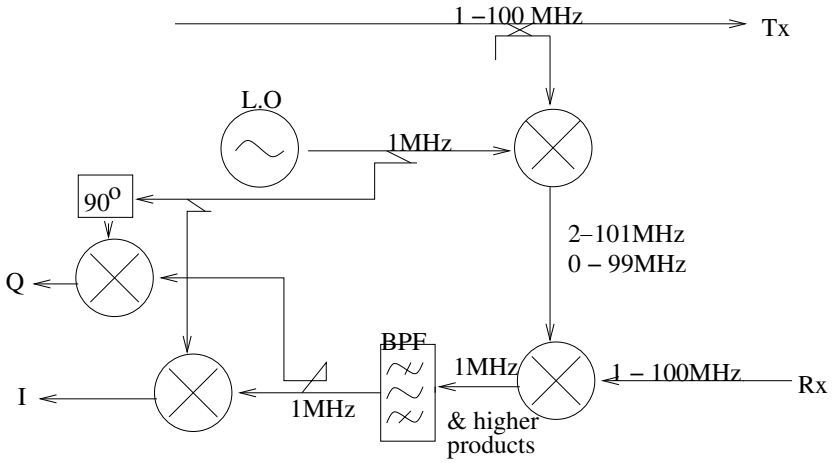

Figure 5.2: Block diagram of a heterodyne architecture.

5.3 Heterodyne Receiver Simulation

For reasons explained above a single conversion heterodyne architecture was simulated. The block diagrams of figure 5.2 and figure 5.3 shows the values that were used for the simulation. The receiver simulation design can be split into three interdependent stages as follows:

- the Radio frequency (RF) stage, and
- the intermediate frequency (IF) stage.
- the demodulation stage (discussed in section 5.5)

Figure 5.3 shows these three stages in block diagram form. The three stages are briefly discussed below and their simulations presented subsequently.

5.3.1 Radio Frequency (RF) Stage

The RF stage of a heterodyne receiver typically consist of a low-noise RF amplifier and a *preselect* bandpass filter. A *preselect* filter is usually placed ahead of the first RF amplifier, set to the RF

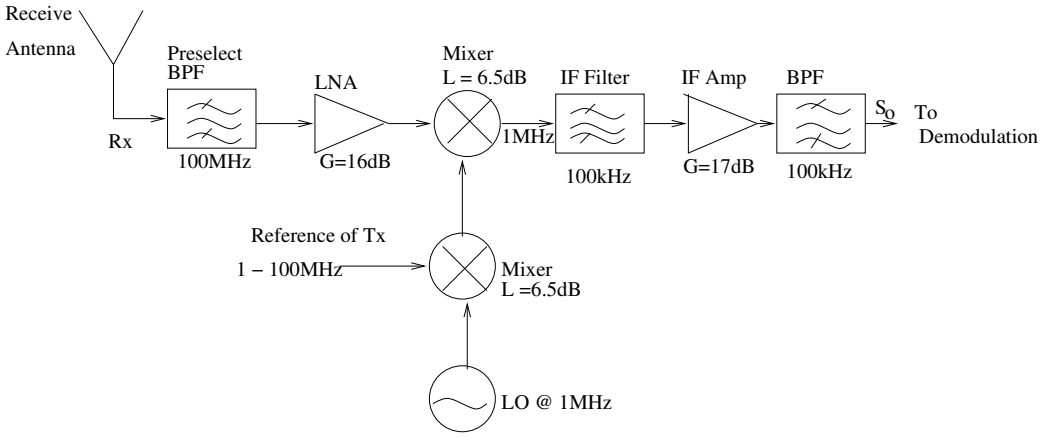

Figure 5.3: Block diagram of the Receiver chain.

tuning range of the receiver. The function of the *preselect* filter, amongst others, is to reject out-of-band interference, which is particularly important for preventing strong interference signals from saturating the RF amplifier or mixer. The noise figure of this filter must be kept as low as possible, in order to reduce the total noise figure of the system. This means the cutoff characteristics of this filter will not be sharp, and therefore will not provide much rejection of the image frequency.

5.3.1.1 Simulation of the Radio Frequency Stage

Preselect Bandpass Filter

To simulate this stage of the receiver, the above theory was used. Since the received signals from the receive antenna cover the frequency range from 1MHz to 100.2MHz, giving a spectrum of 99.2MHz. The preselect bandpass filter was made to have a low cutoff frequency of 950 kHz and high cutoff frequency of 101.2 MHz, which is a bandwidth of 100.25 MHz. This filter was design to have a gain of 0dB and 2 dB insertion loss, to avoid amplifying the noise and image frequencies. A Butterworth 3 pole filter was used. This is because not a very sharp cutoff was needed in this stage, only the maximally flat response that it provides was of interest.

Low Noise RF Amplifier

For the frequency range of 1MHz up to 100 MHz, a suitable low cost amplifier to use in the RF front-end is the GALI-52 Mini-circuit monolithic amplifier [16]. The specifications of this GALI-52 amplifier are as follows:

Frequency(MHz)	Gain (Min)	Output (1dBComp.)	Noise Figure (dB)	IP3	Power Max.
$f_U - f_L$	G(dB)	dBm	dB	(dBm)	P(mW)
DC-2000	16	15.5	2.7	32	350

Table 5.1: GALI-52 Low Noise RF Amplifier Specifications

The noise figure of the receiver is primarily dependant on the noise figure of the first stage [17]. However if the gain of the first stage is not sufficient, a high noise figure of the successive stage will increase the receiver noise figure significantly [6, 7].

5.3.2 Intermediate Frequency Stage

In the IF stage, the bandpass filtered output of the low-noise amplifier is down-converted to an intermediate frequency. A reference of the transmitted frequency is mixed with the local oscillator frequency f_{L0} . This RF mixing signal is then used to drive the receiver mixer. Thus the received frequency f_{Rx} is mixed by $f_{Tx} \pm f_{LO}$, the transmit frequency offset by the IF frequency. The output of the receiver mixer will consist of the two difference terms added at the IF and the two sum terms which are rejected by the IF filter. The local oscillator, the transmitted and received frequencies for the simulation are shown in figure 5.2.

5.3.2.1 Simulation of the Intermediate Frequency Stage

Down-conversion Mixer

The theory above was used to down-convert the RF signal to an IF of 1 MHz. The mixing system consisted of two monolithic mixers. ADE-3L Mini-Circuits mixers were used for both the reference mixer and the receive mixer.

For the reference mixer: A local oscillator at 1 MHz was mixed with a reference of the transmitted signal at the frequency range of 1-100 MHz. The reference mixer choice, took into account that, the performance of a mixer starts to deteriorate towards the upper frequency range. In Mini-Circuits, the conversion loss of the mixer was specified to have an average of 6.6 dB.The performance of the receiver system was based on the output SNR, the receiver dynamic range, the MDS The frequency range was specified as 1-100 MHz for the LO/RF ports and DC-100 MHz for the IF port. The RF port of the reference mixer was at 0 dBm . The local oscillator port was at 10 dBm , thus a local oscillator power of 10 dBm was specified in Mini-Circuits.

For the receive mixer: this mixer was driven by two sideband on the local oscillator port and the received signal at the RF port. The RF port was connected to the output of the GALI-52 low-noise front end amplifier. The output of this mixer, that is the IF signal, was at 1 MHz and higher frequencies.

Frequency MHz	Frequency MHz	Conversion Loss	LO-RF Isolation	LO-IF Isolation
LO/RF	IF	Mid-Band	dB	dB
0.2-400	DC-400	6.5	50	50

Table 5.2: ADE-3L Mini-Circuits Mixer Specifications

Frequency(MHz)	Gain (Min)	Output (1dBComp.)	Noise Figure (dB)	IP3	Power Max.
$f_U - f_L$	G(dB)	dBm	dB	dBm	mW
DC-3000	17	12.7	3.7	27	330

Table 5.3: VAM-93 Mini-Circuits IF Amplifier Specifications.

The same reference mixer specifications were used for the receive mixer. The specifications for the mixer are as shown in table 5.2.

The IF Filter

The output of the receive mixer was filtered by a bandpass filter such that the higher frequencies were rejected. The output of the filter was a signal with a carrier frequency at 1 MHz. A filter with a bandwidth of 100 kHz and insertion loss of 5 dB was simulated in SystemView. It was done using a three pole Butterworth with a cutoff at 950 kHz and 1.05 MHz. Therefore the bandwidth of the IF filter was 100 kHz. Another filter that would be suitable for this task would be a Bessel filter, because of its sharper cutoff compared to the Butterworth.

The IF Amplifiers

Because of lower gain in the LNA and the losses in the mixer, the gain of one amplifier was not sufficient to optimise the dynamic range of the receiver. It was therefore noted that, two IF amplifiers one of 17 dB and the other of 12.6 dB and one final IF filters described above were needed to drive the output of to the desired 0 dBm. VAM-93 Mini-Circuits operational amplifiers with a fixed gain of 17 dB at 1 MHz were used. The specifications for the two IF amplifiers are shown in table 5.3. The specifications for the two amplifiers are similar, the only difference being the gain and that the 12.6 dB amplifier is called the VAM-90 in Mini-Circuits.

5.3.3 The IF I-Q Demodulation Stage

The output of the receiver chain was demodulated into the In-phase and Quadrature channels. The aim of the demodulation is to ensure that both the phase and amplitude information about the target is retained. Here the output signal is split into narrow baseband I and Q channels. Each channel is then sampled using a high precision , low speed digitiser [3].

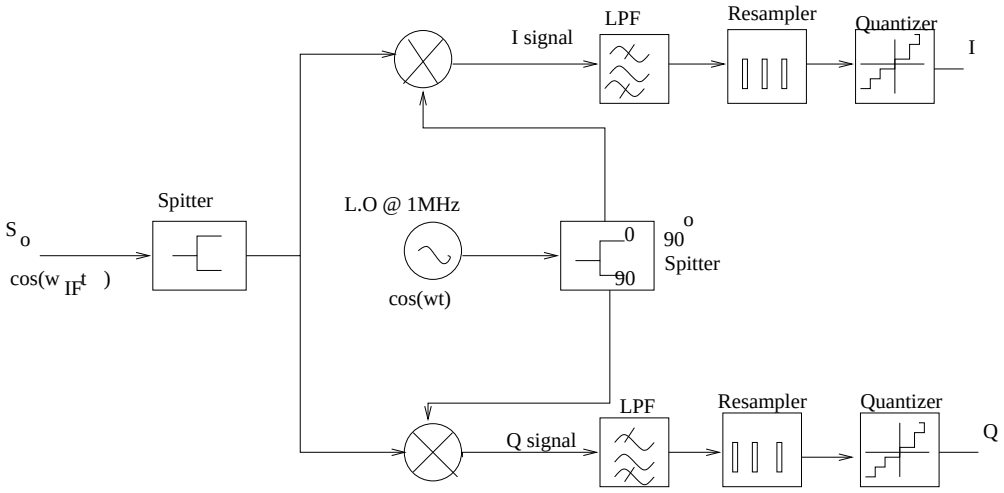

Figure 5.4: Diagram showing how the I-Q Demodulation in SystemView was achieved.

5.3.3.1 Simulation of the Demodulation Stage

The output of the receiver chain was demodulated into the In-phase and Quadrature channels as shown in figure 5.4 . SystemView does not have a I-Q demodulator, thus a group of tokens were assembled together to simulate the demodulator. The final output IF signal from the IF filter, was split into two similar signals using a SystemView splitter PSplitter-2. Because the output signal is at 1 MHz, the local oscillator shown in figure 5.3 was used for demodulation. The one signal was demodulated with a local oscillator signal, that is $cos(\omega_{IF}t_n)$, to produce the In-phase. The other signal was demodulated using the 90^0 phase shifted local oscillator signal, that is $sin(\omega_{IF}t_n)$, to produce the Quadrature signal. This means that the reference of the local oscillator was split into two signal, one of them shifted by 90^0. The two I and Q signals were lowpass filtered using a 3 pole Butterworth IIR filter with a cutoff frequnecy of 1.05 MHz. The I and Q time representation before the quantisation of the signals is shown in figure 5.5 for the first three frequencies.

5.3.3.2 Analogue to Digital Conversion or Quantisation

The analogue to digital conversion was done using a quantiser. In SystemView a quantiser performs the same task as the analogue to digital converter. But is simpler because the quantiser does not need clock synchronisation. The I and Q signals have a quoted minimum signal value of -2.686 mV and -2.441 mV respectively. And a quoted maximum value of 5.371 mV and 18.42 mV respectively. The I and Q signals have a quoted mean noise value of $7.201 \times 10^{-2} mV$ and $4.682 mV$ respectively. A 14 bit quantiser with a voltage span of 2 V was used. The stepsize of the quantiser therefore was $a = \frac{V_{span}}{2^{14}} = 122 \times 10^{-3} mV$ and the number of quantisation levels is $2^{14} - 1 = 16383$. To be able to do signal integration of the system, the thermal noise must be greater than $a/2$. The minimum noise value was $7.201 \times 10^{-2} mV$ which is greater than $61.035 \mu V$. When no signal was present the

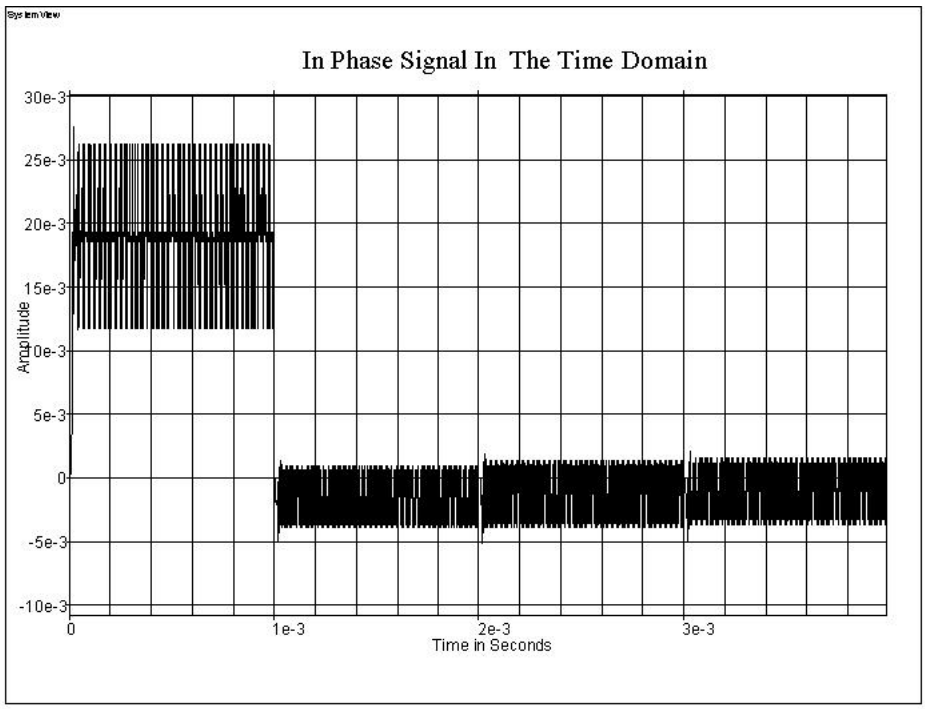

(a)

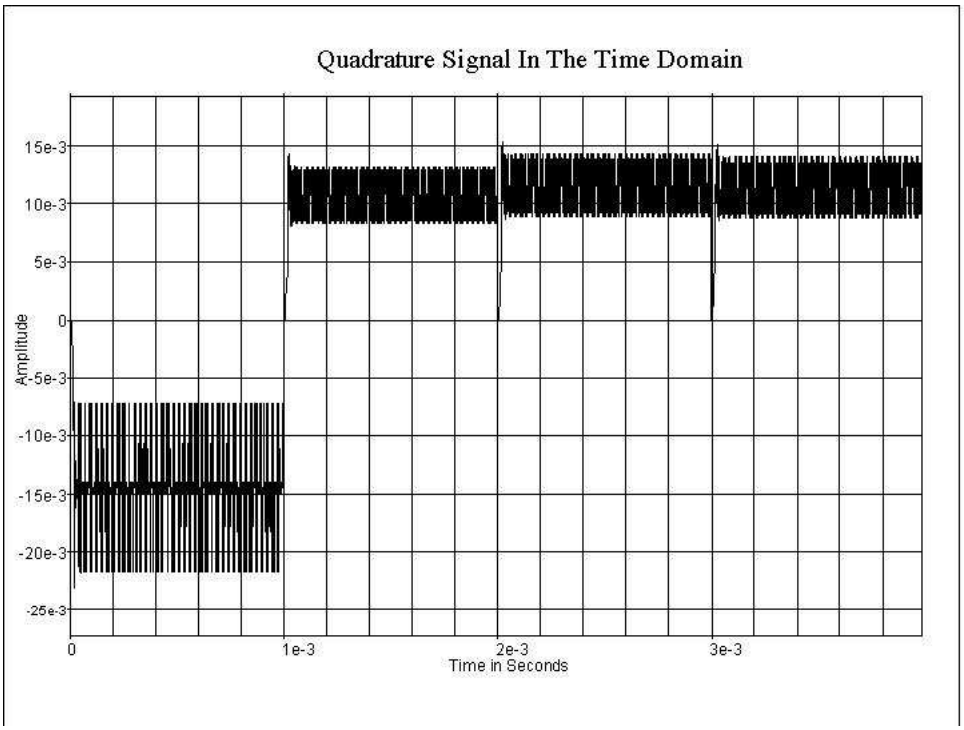

(b)

Figure 5.5: The In-phase and Quadrature time domain plots before the quantisation or digitisation.

noise toggled the quantiser and it sampled even when no signal was present. The output data values of the quantiser were then taken to Matlab for further signal processing. A SystemView diagram of the completed receiver is shown in Appendix C. The range profile plots of Matlab are also shown in Appendix C.

5.4 Receiver Performance

The performance of the receiver system was based on the output SNR, the receiver dynamic range, the MDS. The purity of the power spectrum of the output signal was also observed. Figure 5.6 show the output spectrum of the receiver given that the transmitted signal was 10 dBm and the medium was 10 dB. The power of the output signal was observed to be -7 dBm. The I and Q plots show an average noise of 7.201x10^{-2} [mV] as as input to the quantiser. Thus the toggles the quantiser to sample even when no input signal is present.

5.4.1 Signal to Noise Ratio

.

5.4.2 Noise Figure

When the receiver simulation was designed above, it was found that more gain was needed in the IF stage in order to optimise the dynamic range of the receiver. It was therefore noted that, two IF amplifiers one of 17 dB and the other of 12.6 dB and one final IF filters described above were needed to drive the output of to the desired 0 dBm. The input signal to noise ratio at the input of the receiver was calculated at $\frac{S_i}{N_i} = 89.54$dB. From the above section the output signal to noise ratio is $\frac{S_0}{N_0} = 126.89$dB with the noise at $N_0 = -126.9$dBm, all being system values. Thus the noise figure is $\frac{S_i/N_i}{S_0/N_0} = -37.356$dB. This value of the noise figure does not make sense. The long hand-calculation of the noise figure gives

$$F = F_1 + \frac{F_2 - 1}{G_1} + \frac{F_3 - 1}{G_1 G_2} + ... = 5dB$$

where $F_1 = 2.7$dB and $G_1 = 16$dB. The long hand calculation gives a noise figure better than the specifications requirements. This is the genuine noise figure of the system for the following reason. The writer found that the dBm values of SystemView are in essence dB. Because of that error in the SystemView analysis window, the successive mean, minimum and maximum values for the noise

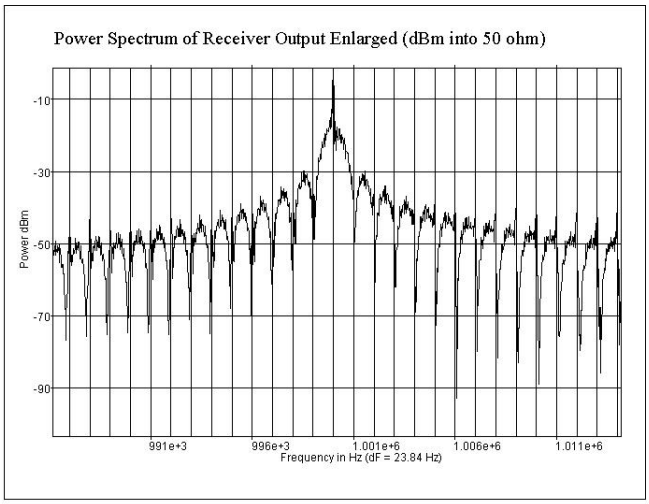

(a)

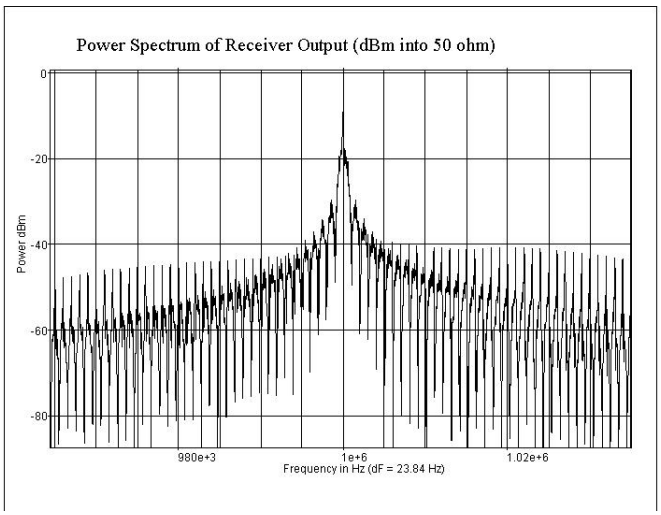

Figure 5.6: Power Spectra at the receiver output.

and signal are circumstantially erroneous. However, the writer decided to use the SystemView noise figure value for the rest of the receiver analysis for simplicity reasons.

5.4.3 Compression and Third-Order Intermodulation

The power levels that exceed the 1 dB compression point P_1 of an amplifier will cause harmonic distortion and power levels in excess of the third order intercept point P_3 will cause intermodulation distortion. Therefore it is important to track the power levels through the stages of the receiver to ensure that P_1 and P_3 are not exceeded. This was conveniently done with a graph of the form shown in figure 5.7. It was found that the P_1 and P_3 of the amplifiers and mixer were not exceeded as shown in the figure 5.7.

The third-order intercept point P_3 was taken as the smallest of all the components in the system since that is the minimum P_3 that should not be exceeded by the signal. Similar analogy was used for P_1 . Thus the values for P_1 and P_3 respectively are 12.7 and 27 dBm. The P_3 values are not shown in figure 5.7, because they are well above the P_1. If P_1 cannot be exceed, P_3 cannot be exceeded as well.

5.4.4 Receiver Dynamic Range

The linear dynamic range of the system was calculated at

$$DR_l = P_1 - N_0 = 12.7 - (-126.9) = 139.6dB$$

The spurious free dynamic range was calculated at

$$DR_f = \frac{2}{3}(P_3 - N_0 - SNR) = \frac{2}{3}(27 - (-126.9) - 119.9) = 22.67dB$$

5.5 Summary

This chapter can be summarised as follows. A heterodyne architecture was chosen because the homodyne architecture has limitations that the heterodyne easily overcome. Thus the receiver simulation was a single conversion heterodyne with three stages. The first stage was the RF stage with a preselect filter of 100MHz bandwith and a Mini-Circuit GALI-52 LNA RF amplifier. The function of the *preselect* filter is to reject out-of-band interference, which is particularly important for preventing strong interference signals from saturating the RF amplifier or mixer.The second stage, the IF stage, the bandpass filtered output of the low-noise amplifier is down-converted to an intermediate frequency.

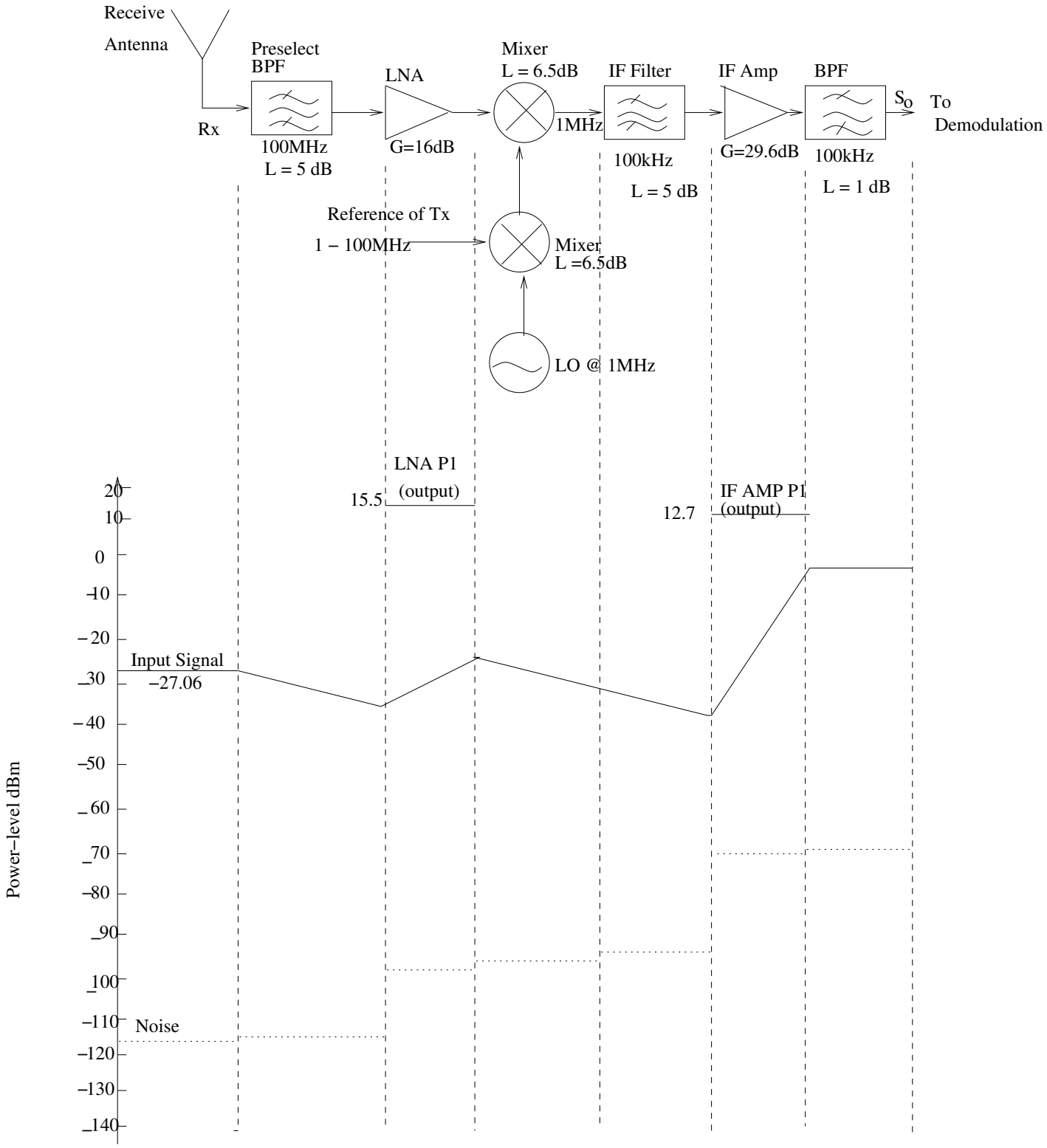

Figure 5.7: Diagram of noise and signal at consecutive stages of the receiver.

A reference of the transmitted frequency is mixed with the local oscillator frequency f_{L0} . This RF mixing signal is then used to drive the receiver mixer. Thus the received frequency f_{Rx} is mixed by $f_{Tx} \pm f_{LO}$, the transmit frequency offset by the IF frequency. The output of the receiver mixer will consist of the two difference terms added at the IF and the two sum terms which are rejected by the IF filter. The two mixers used in the simulation were Mini-Circuit ADE-3L mixers with a conversion loss of 6.5 dB. The bandwidth of the IF filter was 100 kHz. This filter was designed in SystemView using a three pole Butterworth filter with a cutoff at 950 kHz and 1.05 MHz. The output of the filter was a signal with a 1 MHz carrier frequency. The third stage was the demodulation stage where the 1 MHz signal was demodulated into In-phase and Quadrature components using the local oscillator signal. The 1 MHz was split into two equal signals using SystemView's power splitter. The two signals were then mixed with local oscillator at 1 MHz to baseband using ADE-3L mixers. The basebanded signals were then digitised using high precision and low speed 14 bit quantisers. The data was kept into a file for further analysis in Matlab. The performance of the receiver was then conducted based on the SNR, the third-order intermodulation and the dynamic range.

Chapter 6

The Comparison of SFCW GPR to Impulse GPR

6.1 Introduction

In this chapter the results of the comparison simulated SFCW GPR system will be presented. In chapters 3, 4, and 5 the performance of the transmitter, the medium and the receiver was discussed and results with regard their performance were shown. For the transmitter, its performance is investigated in section 3.6. The propagation medium performance is shown in section 4.4. The receiver performance is tested section 5.4. Therefore those results will not be repeated in this chapter.

For comparison purposes, both the Impulse and SFGPR radar systems were modified to have the same propagation medium characteristics. Further modification that was made to the existing SFCW system is described in section 6.2. The modified SFCW GPR system performance is discussed in section 6.3. A summary of how range profiling and what it means is included followed by range profiles of the two systems in section 6.5. The last section briefly summarise the performance of the SFCW GPR compared to the Impulse GPR.

6.2 Modifying the existing system

When the SFGPR system performance was compared to the Impulse radar system the following modifications were made to the SFGPR.

- The system was simulated to do 50 profile per second, with each profile made up of 64 frequencies. The number of frequency steps *n,* was equal to 64. The 64 frequencies were transmitted for a total of 20 milliseconds, such that 50 profiles were taken in one second. This required that

each frequency be transmitted at most for a dwell time, $T_{dwell} = 20x10^{-3}/64 = 312.5\mu s$. For the first carrier frequency, $f_0 = 1MHz$, the period is $T_0 = 1000ns$. Therefore the dwell time of $312.5\mu s$ was adequate to allow a few cycles of each frequency to be transmitted as explained in subsection 3.4. Thus the stop time in SystemView was set at the dwell time value to allow 50 profiles to be taken per second.

- The total radar bandwidth was made 100 MHz for the 64 frequencies transmitted. This resulted in a calculated frequency stepsize of $\Delta f = B_{tot}/(n-1) = 1.5873MHz$. The theoretical range resolution of the system therefore was $\Delta R = 611.96mm$ for the same relative permittivity ε_r . The theoretical unambiguous range for the medium was $R_{unam} = 37.95m$, which is 18.79 m better than for the above system which had 32 frequency steps. The range bin spacing was calculated at $\Delta z = 602.4mm$.

- The IF filter bandwith was not changed, it was 100 kHz. The digitisation of the analogue signal was being performed by a 14 bit quantiser. The quantiser was set to take 129 sample per frequency which required a sample rate of 407.6 kHz . The quantiser sample rate did not change the system sample rate which was 400 MHz.

- The transmit signal power was 10mW into 50 ohm and the receiver was simulated to have a noise figure of 5dB.

6.3 Testing The Modified System

The modified system performance was tested for the signal to noise ratio and the minimum detectable signal and dynamic range. The test results are shown below.

Signal to Noise Ratio

The performance of the modified system was tested briefly as follows. First to ensure that the transmitted signal had a power level of 10 dBm, the power spectrum of the transmitted signal was observed figure 6.1 (a). The transmitted signal propagated into a 10 dB attenuative medium. The input to the receiver, which is the output form the medium is shown in figure 6.1 (b). From the two plots, the sidelobes are very tightly packed and narrower, because the number of frequency steps was increased and the frequency stepsize decreased. At a carrier frequency of 1 MHz, the first transmitted and received signal peaks. Theoretically, a 10 dB attenuator with an input power of 10 dBm, has a 0 dBm power output.

Practically, the signal at the output of the medium was not zero but -7.129 dB. The SNR of the input to the receiver was calculated at $SNR_i = S_0 - N_0 = -7.129 - (-83.47) = 76.34$ dB. The received

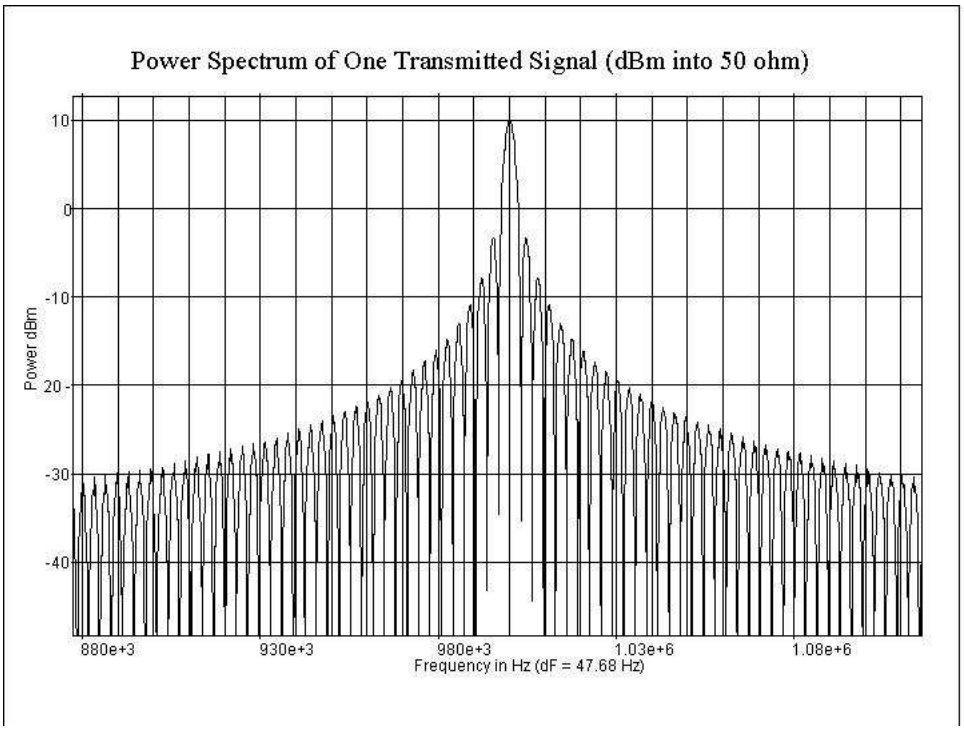

(a)

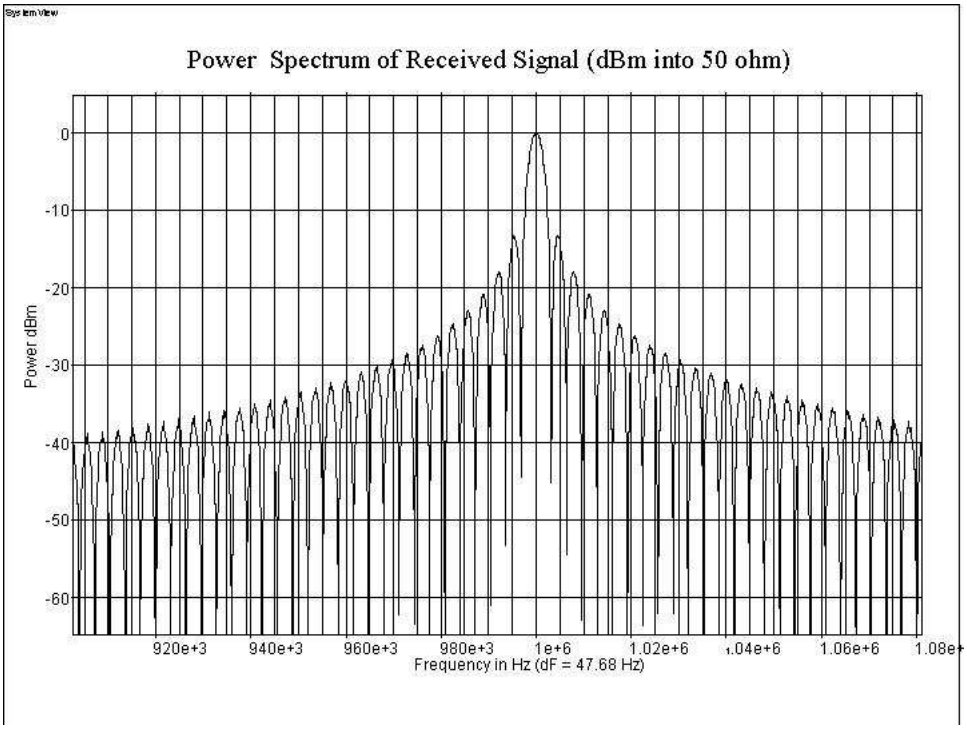

(b)

Figure 6.1: Figure 6.1 (a) shows the transmitted spectrum of the first transmitted signal. Figure 6.1 (b) shows the received spectrum with a power level close to zero.

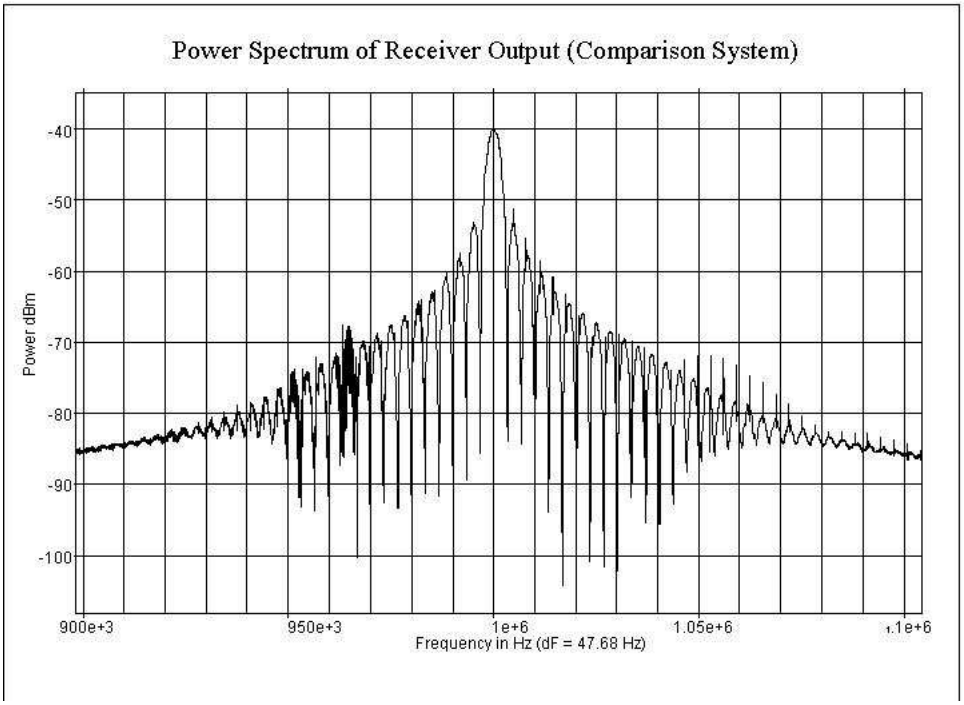

Figure 6.2: Power Spectrum of the Receiver Output.

signal entered the receiver described in section 5.3. The output power spectrum at the receiver chain is shown in figure 6.2

The output power spectrum of this system had a peak power level of -40 dBm at 1 MHz. The SNR at the output is 101.3 dB, with the mean noise value at the output being $N_0 = -141.3$dBm. Thus the noise figure of the receiver was $F = SNR_i - SNR_0 = 76.34 - 101.3 = -24.959$ dB. This was another error by SystemView. Notice that adding 30 dB to this value gives 5 dB. This also proves that the SystemView analysis window is giving erroneous values in dBm.

Minimum Detectable Signal

The minimum detectable signal calculated from the above values and from the fact that $P_1$and P_3 equal to 12.7 and 27 dBm, *see* 5.4.3, is shown here. The linear dynamic range was calculated at $DR_l = 154$ dB and the spurious free dynamic range was calculated at $DR_f = 44.67$ dB.

I-Q Demodulation

The output signals at the output of the I and Q channels are shown in figure 6.3. The time domain plots shown here are at the input of the quantiser, before quantisation. The important aspect of this figure is the average signal and noise voltage. The average noise voltage is important because it toggles the

quantiser. As explained in subsection 5.3.3.2, a 14 bit quantiser with a 2 V voltage span has a stepsize $a = \frac{V_{span}}{2^{14}} = 122 \times 10^{-3} mV$. To be able to do signal integration of the system, the thermal noise must be greater than $a/2$. The minimum average noise value between I and Q for this system was $1.879 \times 10^{-1} mV$ which is greater than $a/2$. This is done so that signal averaging in post processing can be possible. The peak quantisation power for this system is $P_{qnt,pk} = 30 + 10log(\frac{a^2/12}{50}) = -16.05[dBm]$.

6.4 Range Binning

The first step in the computer processing of the stepped frequency signals is range binning, that is organising the data in a range-frequency matrix. Each of the 64 frequencies has 129 samples of it taken both in the I and the Q channel. Each sample is a number. In each frequency an average value of the sample numbers was taken for each I and Q. Since there are 64 frequency steps, it means 64 averages were taken forming 64 complex samples $I + jQ$. This is shown below for only f_0 , f_1 and f_2 of the I channel.

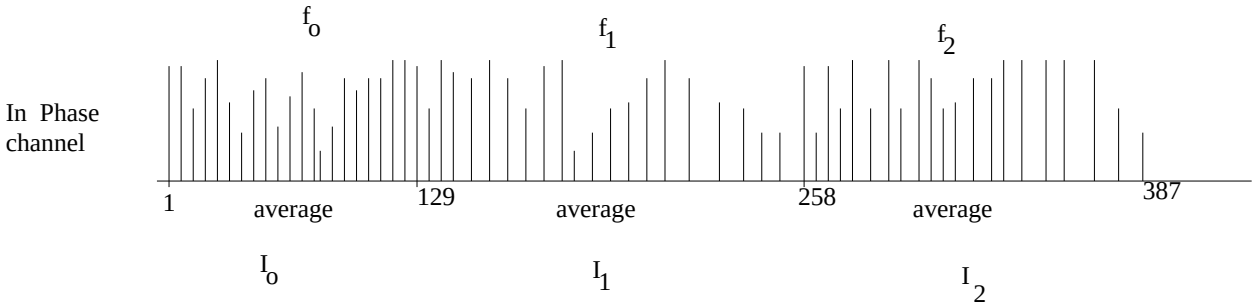

Figure 6.4: This figure shows the number of samples that are taken for each frequency. An average of the sample values is then taken which gives one I value. This figure only depicts three frequencies.

These complex samples form an array with 64 rows. The inverse fast Fourier transform of these complex was taken and the time plot is called the high range resolution profile. The number of frequencies is in the x-axis of the plot and the y-axis represent the magnitude of the IFFT.

6.5 Range Profiling

The final step in the processing of the stepped frequency signal is range profiling. This was also done using Matlab. The Matlab code shown in Appendix D, was used to plot the range profiles for this comparison system. The formula of subsection 3.6.4 was used to plot the range profile. This was done in Matlab. The Matlab code is included in apppendix D. Figure 6.5 shows the range profiles of

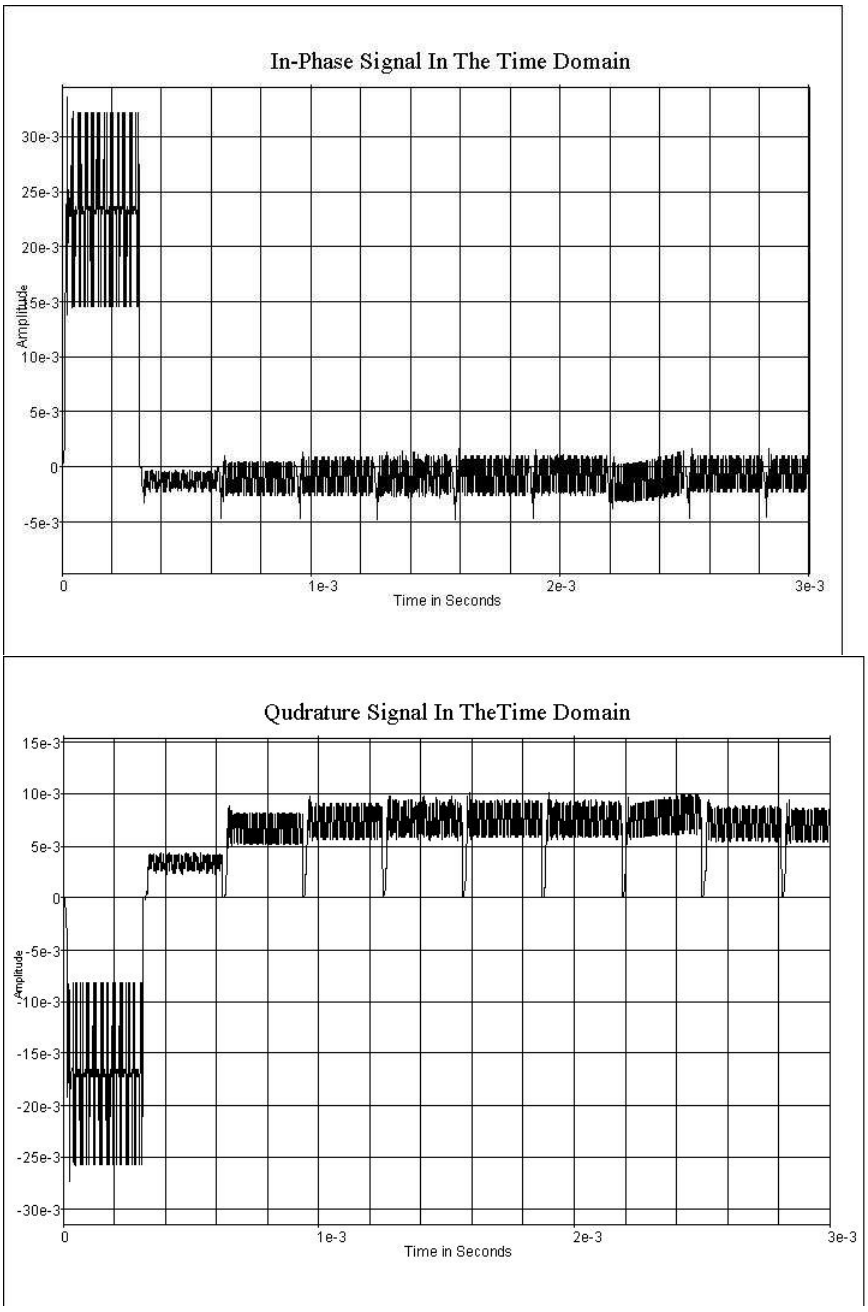

Figure 6.3: The time domain representation of the I and Q signals before quantisation.

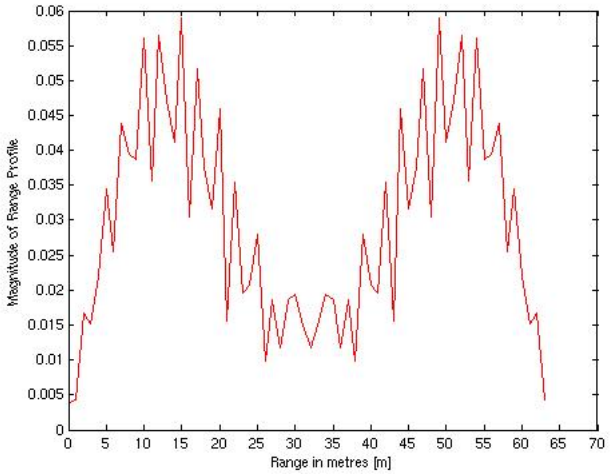

(a)

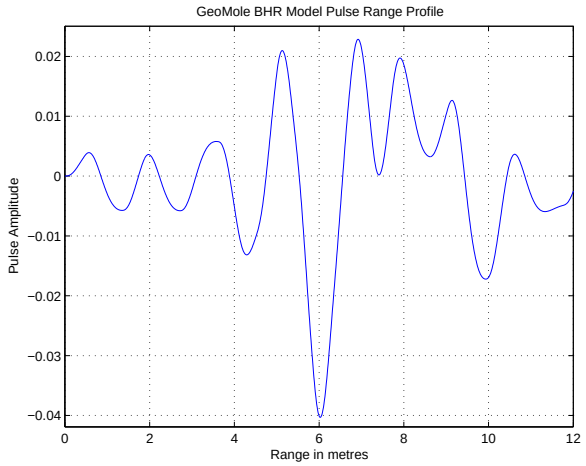

(b)

Figure 6.5: The Range Profiles of both the SFCW GPR and the GeoMole BHR Impulse radar systems.

Transmitted Power, P_t	Generated Power P	Transmitter Bandwidth	Pulse Repetitive Period
26 dBm	48 dBm	100 MHz	550 ns
Transmitted Voltage V_p	Generated Voltage V_p	Pulse Repetition Frequency	Pulse width
-65.29 V	1000 V	1.8018 MHz	8 ns

Table 6.1: GeoMole Transmitter Specifications

Gain	Bandwidth	Noise Figure	Dynamic Range	Penetration Depth	Range Resolution
	100 MHz	5 dB			

Table 6.2: GeoMole Receiver Specifications

the SFCW and the impulse system. Because zero padding was not done for the SFCW shown here, the smooth peaking of the sinusoid with noise is now shown as noise. This was done so as to show the effect of zero padding in signal processing. Plots are included in Appendix D that show a zero padded signal and a signal that is not zero padded. With zero padding, the signal would be smooth. The peak signal value at R = 15 m was V_p =0.055 and the average noise is V_{rms} =0.015 for the SFCW. From figure 6.5 (b) it was noted that the peak signal value at R = 5 m was 0.02 and the average noise is 0. The peak signal to noise power for the SFCW is therefore $PSNR = V_p^2/V_{rms} =$

6.6 GeoMole BoreHole Impulse Radar Specifications

The reader is referred to a dissertation by Guma et al [4] for the simulation, discussion and performance testing of the GeoMole BHR impulse radar system referred to here. The transmitter and receiver specification values for the GeoMole impulse radar are summarised in tables ?/ and ?/.

6.6.1 GeoMole Impulse Radar Transmitter

6.6.2 GeoMole Impulse Radar Receiver

6.7 SFCW GPR vs GeoMole BHR Impulse GPR

From table 6.2, the impulse radar has a receiver dynamic range of 74.8 dB and the SFCW GPR has a dynamic range of 154 dB . The comparison between the SFCW and the Impulse is shown in table 6.3. The stepped frequency radar transmits the smallest power but still proves to be the better system.

	SFCW GPR	GeoMole BHR Impulse GPR
P_t	10 dBm	26 dBm
L	10 dB	10 dB
SNR_0	101.3 dB	5.09 dB
DR_l	154 dB	74.8 dB
DR_f	44.67 dB	47.47 dB
R_{max}	15m [no stacking]	13.5 m [no stacking]
P_1	12.7 dBm	13 dBm
P_3	27 dBm	14.5 dBm

Table 6.3: The SFCW versus GeoMole BHR Impulse Radar.

6.8 Summary

The performance of a SFGPR system was found to be better than the impulse system as shown in the table6.3. The SNR and linear DR of the SFCW was better than the impulse. The spurious free dynamic range of the impulse is greater than that of the SFCW. The receiver of the SFCW was seen to have a lower first order compression point, but a higher third-order point. The general SFCW compared to the GeoMole BHR Impulse system was better.

Nonetheless, it was found that stacking of signals was impossible in SystemView for a SFCW since memory ran out. This resulted into stacking not being performed for the SFCW system. It was however found that stacking would possible in Matlab. This was not done because of time constraints. A Matlab code for stacking 64 signals would have consumed much time and affect the completion of the project. The stacking is thus mentioned here for future work.

Chapter 7

Conclusion and Recommendations

Based on the findings of this report and the experience gained during the work, the following conclusion can be drawn:

- A stepped frequency continuous wave ground penetrating radar was simulated using SystemView and found to operate satisfactorily. Several limitations were found and recommendations on an improved second simulation are given.

- A 1-100 MHz CW transmitter was simulated using the variable parameter method, and its performance was tested. The transmitter performance was exceptional well. The spectrum purity of the transmitter led to a good signal to noise ratio at the transmitter output. The phase noise was found not degrading the performance of the transmitter. Even thou not all transmitted signals were observed to have power level of 10 dBm, no frequency jitter was experienced in the transmitter. The transmitter simulation was completed with a transmit antenna simulated with filter models and attenuators.

- The propagation medium simulation was kept simple. A better medium simulation was suggested where the attenuation versus frequency relationship was used. Research had shown that attenuation increases with frequency, this fact was used to suggest an alternative to the simple ground simulation. Furthermore, how this can be done in SystemView was described in great detail.

- A heterodyne architecture receiver system was chosen over the homodyne because of its capabilities. A 1-100 MHz CW receiver using a single IF system was simulated, and its performance tested. The dynamic range of this receiver was measured to be which is less than or greater than . Improvements on the receiver simulation to increase the dynamic range are given in the recommendations.

- The demodulation stage of the receiver was simulated and found to operate satisfactory. The amount of noise signal at the demodulator output was found to be important of signal averaging. The mean noise value was used to toggle the quantiser, so that when signal integration takes place the signal would separates itself from noise.

- A Signal processing code was compiled in Matlab and used to obtain the high range resolution of the radar. The code was found to operate unsatisfactory. The range profile obtained from the code is shown in Appendix D. Improvements on the code are given in the recommendations. The performance of the completed simulation was tested against a Geo Mole BHR impulse radar system. Practically , the performance of the SFCW was found satisfactory. The linear dynamic range of the SFCW was 79.2 dB above the impulse system when the transmit power of SFCW was 10 dBm. The transmit power of the GeoMole Impulse radar was calculated at 26 dBm and the losses in both systems were 10 dB. Also, both systems were simulated to have antenna gains of 0 dB. The overall performance of the SFGPR radar compared to impulse radar system is better.

Based on the findings of this report, the experienced gained through the work and the above conclusions, recommendations on improvements on the system and future work are made. These recommendations should be used to optimise the simulation into the next level.

7.1 Transmit Antenna Improvements

The transmit antenna simulation was merely done using filter models with a gain of 0 dB in the passband for this simulation. It is recommended that , real antenna imperfections used in SFCW GPR, be simulated and incorporated with this design. This will improve the signal to noise ratio at the output of the transmitter even more.

7.2 Propagation Medium

The concept of developed in chapter 4, of the linear relationship between the attenuation and the frequency should be investigated further. Ground models based on that concept will then be simulated and incorporated in the simulation. This will drive the simulation more to the real SFCW GPR simulator.

7.3 Signal Processing

The time extent to which this project could be finished was underestimated. Therefore better signal processing methods could not be covered. It is highly recommended to improve the signal processing code used. Improvements on the code will result in huge improvements in the range profile plots. Because also SystemView runs out of memory when stacking was done, methods that will eliminate this problem can be of great significance.

Bibliography

[1] Alan Langman,"Design of Hardware and Signal Processing for a Stepped Frequency Continuous Wave Ground Penetrating Radar", PhD Thesis, University of Cape Town, March 2002

[2] D.A.Noon, "Stepped-Frequency Radar Design and Signal Processing Enhances Ground Penetrating Radar Performance", PhD Thesis, Univeristy of Queensland,1996

[3] Richard Thomas Lord, "Aspects of Stepped-frequency Processing for Low-Frequency SAR systems", PhD Thesis, University of Cape Town, 2000

[4] G.M. Kahimbaara, "Investigation and Simulation of an Impulse Ground Penetrating Radar Application", BSc. Thesis, University of Cape Town, 2004

[5] D.R. Wehner,"High Resolution Radar", Norwood, MA : Artech House ,1995,

[6] M.I. Skolnik, "Introduction to Radar Systems", McGraw-Hill, New York , USA, 1962

[7] M.I.Skolnik, "Radar Handbook", McGraw-Hill, New York, NY, USA, 1990

[8] Marten Kabutz, "RF Hardware Design of a Stepped Frequency Continuous Wave Ground Penetrating Radar", MSc. Thesis, University of Cape Town, 1995

[9] James D. Taylor, "Ultra Wideband Radar Technology", CRC Press, Boca Raton, FL, 2001

[10] J.C. Fowler, S.D. Hale, and R.T. Houck. Coal Mine Hazard Detection Using Sythetic Pulse Radar. RnMines OFR 79-81,ENSCO Inc., US Bereau of Mines Contract HO292925, January 1981.

[11] Gordon Farquharson, "Design and Implementing of a 200 -1600 MHz Stepped Frequency Ground Penetrating Radar", MSc. Thesis, University of Cape Town, 1999

[12] David M. Pozar, " Microwave and RF Design, John Wiley & Sons, Inc. New York, 2001

[13] A.G. Stove, "Linear FMCW radar techniques", IEE Proc, F, Comm, Radar & Signal Processing,1992

[14] http://fate.clu-in.org/gpr.asp?techtypeid=41

[15] Michael K. Cope, ” Design, Simulation and Implementation of a digital Quadrature Demodulator for a Stepped Frequency Radar”

[16] http:www//minicircuits.com/

[17] S.A. Hovanessian, “Radar System Design and Analysis”, Artech House, Norwood, MA, January 1984

Appendix A

Dynamic Range

A.1 The Dynamic Range

Since thermal noise is generated by almost any lossy realistic component, the ideal linear component does not exist in the sense that its output is always exactly proportional to its input excitation. Thus all realistic components are non-linear at very low power levels due to noise effects. And all practical components become non-linear at high power levels.For instance, in amplifiers the gain tend to decrease for large values of the output voltage, this effect is called *gain compression* or *saturation*. Physically, this is usually due to the fact that the instantaneous output voltage of an amplifier is limited by the power supply voltage used to bias the active device. In either case, these effects set a minimum and maximum realistic power range or *dynamic range* over which a given component will operate as desired.

To quantify the linear operating range of the amplifier, we define the *1dB compression point* as the power level for which the output power has decreased by 1dB from the ideal characteristic. This power level is usually denoted by P_1 , and can be stated in terms of either the input or the output power. That is, either referred to the input or referred to the output. We then define intermodulation distortion.

A.1.1 Intermodulation Distortion

Consider a *two tone* input voltage, consisting of two closely spaced frequencies, ω_1 and ω_2 :

$$v_i = V_0(cos\omega_1 t + cos\omega_2 t)$$

The output voltage will consist of harmonics of the form

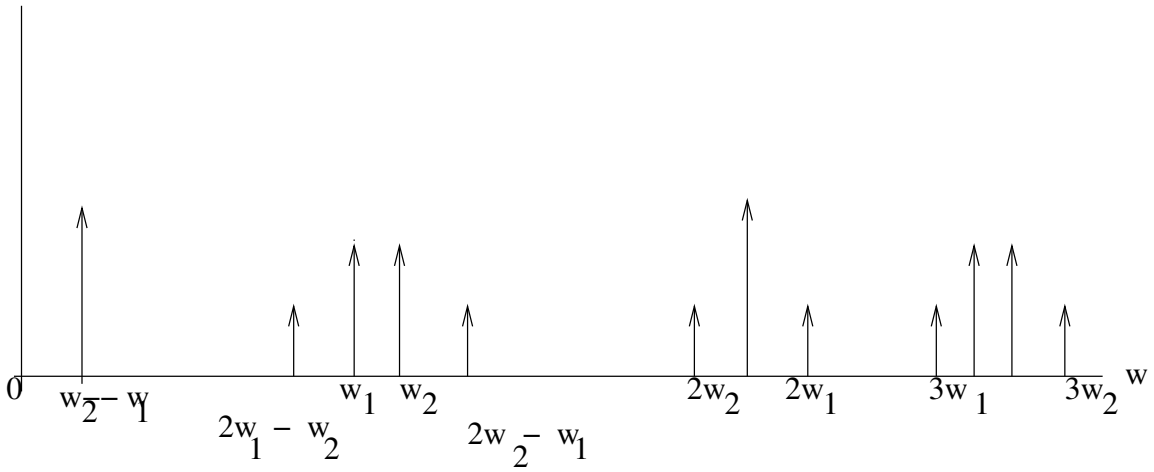

Figure A.1: Output spectrum of second and third order two-tone intermodulation products, assuming $\omega_1 < \omega_2$. This figure was taken from [12], but redrawn by the writer using Xfig.

$$m\omega_1 + n\omega_2$$

with m, n = 0, $\pm 1 \pm 2$ ± 3,.....These combinations of the two inputs frequencies are called *intermodulation products*, and the *order* of a given product is defined as $|m| + |n|$. All the second order products are undesired in an amplifier, but in a mixer the sum or difference form the desired outputs. In either case, if ω_1 and ω_2 are close, all the second-order products will be far from ω_1 or ω_2, and can easily be filtered (either passed or rejected) from the output of the component.

The cube term leads to six intermodulation products: $3\omega_1, 3\omega_2, 2\omega_1 + \omega_2, 2\omega_2 + \omega_1, 2\omega_1 - \omega_2$ and $2\omega_2 - \omega_1$. The first four of these will be located far from $\omega_1$and ω_2 and will typically be outside the passband of the component. But the two difference terms produce products located near the original input signals as shown in figure A.1 , and so cannot be easily filtered from the passband of an amplifier. Figure A.1 shows a typical spectrum of the second- and third-order two tone intermodulation products. For an arbitrary input signal consisting of many frequencies of varying amplitude and phase, the resulting in-band intermodulation products will cause distortion of the output signal. This effect is called *third order intermodulation distortion*. Finally we define the third-order intercept point.

A.1.2 Third-Order Intercept Point

The output power of the first order, or linear product, is proportional to the input power and so the line describing this response has a slope of unity before compression. The line describing the response of the third-order products has a slope of three. The second-order products are outside the passband, therefore do not affect the response. The linear and third -order responses will exhibit compression at

high input powers, we show the extension of their idealised responses with dotted lines. Since the two lines have different slopes, they will intersect at a point above the onset of compression, as shown in the figure. This hypothetical intersection point, where the first order and third order powers are equal is called the *third-order intercept point*, denoted P_3 , and specified as either an input or an output power.

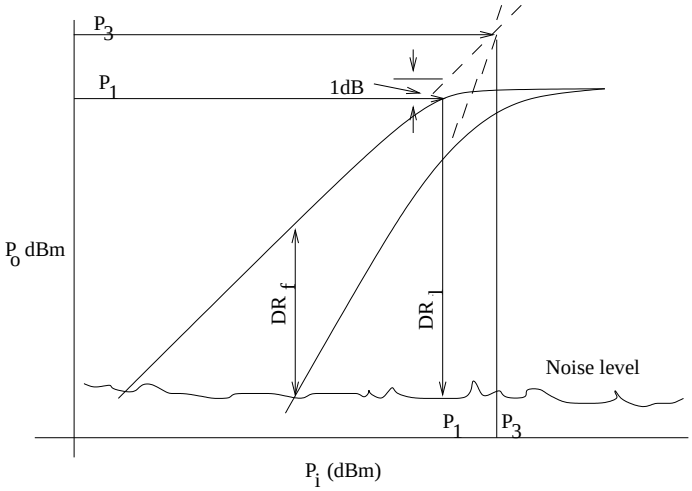

Figure A.2: Illustrating linear dynamic range and spurious free dynamic range. This figure was taken from [12] , and redrawn by the writer using Xfig.

The *linear dynamic range* of a power amplifier, therefore will be, the power range that is limited at the low end by noise and at the high end by the 1dB compression point. That is, $DR_l = P_1 - N_0$. For low-noise amplifiers, operation may be limited by noise at low end and the maximum power level for which intermodulation becomes unacceptable. The *spurious free dynamic range* is defined as the maximum output signal power for which the power of the third-order intermodulation product is equal to the noise level of the component. That is $DR_f(dB) = \frac{2}{3}(P_3 - N_0)$.

A.2 Receiver Dynamic Range

The linear dynamic range and spurious free dynamic range described above are useful in the context of characterising an individual component. The receiving system dynamic range involves the minimum detectable signal power, which is dependent on the type of modulation used in the receiving system, as well as the noise characteristics of the antenna and receiver. The receiver dynamic range is defined as

$$DR_r = \frac{maximum\ allowable\ signal\ power}{minimum\ detectable\ signal\ power}$$

where the minimum detectable signal is defined as

$$S_{i_{min}} = kB(T_a + T_e)(\frac{S_0}{N_0})_{min}$$

and T_a is the antenna temperature, T_e is the equivalent temperature of the receiving system, and $(\frac{S_0}{N_0})_{min}$ is the minimum SNR required for that application. This appendix is an extract from Pozar et al [12] , summarised by the writer.

Appendix B

SystemView Figures

Because SystemView does not support copy of its token figures into Lyx. The SystemView token figures were printed separately.

Figure B.1 is the simulation of the transmit antenna system, showing also the sinusoid that generates the SFCW.

Figure B.2 is the figure showing demodulation.

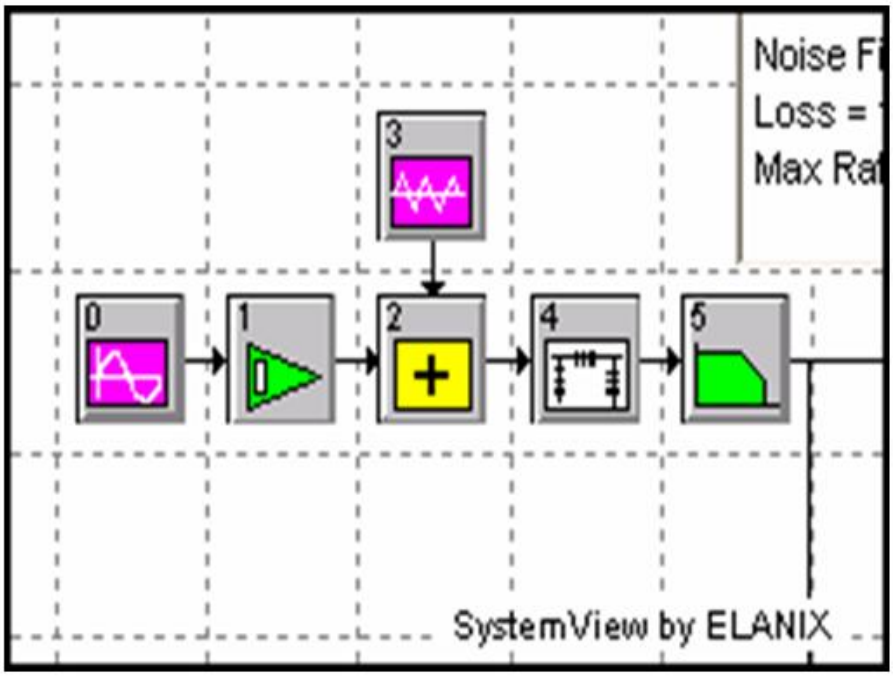

Figure B.1: SystemView Transmit Antenna

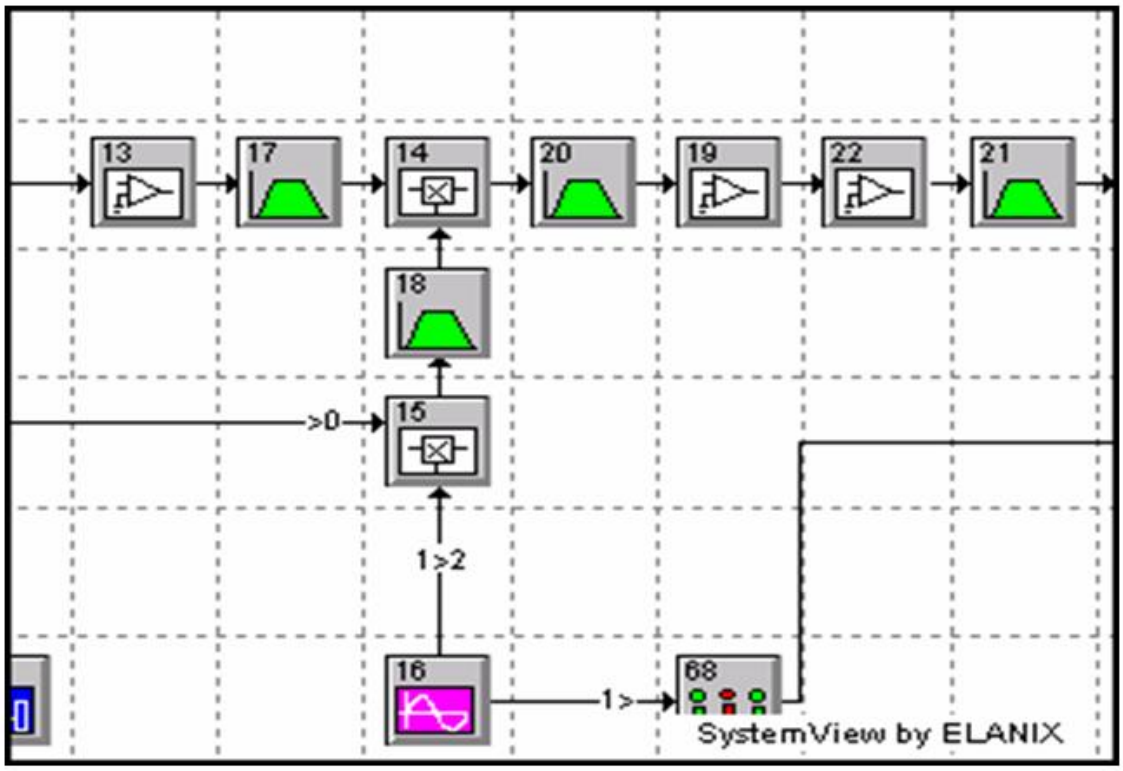

Figure B.2: Receiver showing the down-conversion of the RF signal. The reference is mixed with the local oscillator and the output mixed with the received signal.

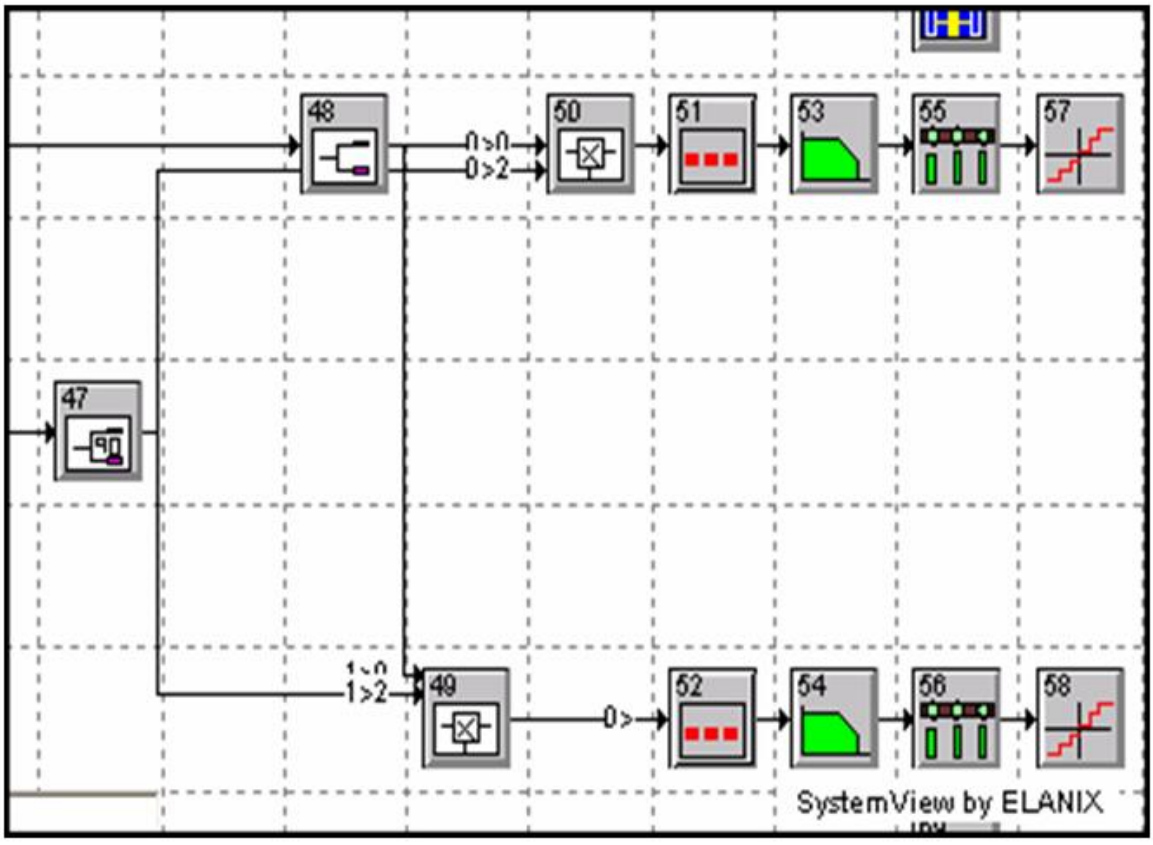

Figure B.3: Demodulation in SystemView.

Appendix C

Matlab Signal Processing

This is a Matlab code that was used to compute the average value per frequency for the I channel. The code below was used in the comparison system of chapter 7, hence 64 frequencies. All these Matlab code were compiled with the assistance of Guma Kahimbaara.

```
% this code computes the average sample
%value per frequency for the I channel
%there should be 64 average values since
%there are 64 frequencies per channel
I = Finalvalue_3pulses_Iout;
N =64; %Number of frequency steps
n =129; %Number of samples per frequency
Sv =0;  %sum of all sample values per frequency
Sav = []; %average sample value for 129 samples
for i =1:N
  for j = 1+((i-1)*129):129+((i-1)*129)
      if j < 8193
      Sv = Sv + I(j,2) %jth row second column
      end
  end
  Sav(i)= Sv/129;  %taking the average value of the sum
  Sv = 0;
end
Sav
```

A similar code was used to obtain the 64 average values for the Q channel. The difference being the data values that were used.

```
Q = Finalvalue_3pulses_Iout;
N =64;
n =129;
Sv =0;
Sqav = [];
for i =1:N
   for j = 1+((i-1)*129):129+((i-1)*129)
        if j < 8193
        Sv = Sv + I(j,2)
        end
   end
  Sqav(i)= Sv/130;
  Sv = 0;
 end
Sqav
```

When the 64 I and Q channels average samples were taken, a complex I +j Q was formed. The magnitude response of the inverse FFT of the complex samples was then plotted as follows:

```
%this code forms the 64
&complex samples I+jQ
%plots the absolute value of
%the ifft for the 64 frequencies
%this is what we call the high
%resolution range profile
p = 8192;% does the zero padding
&to obtain a smooth plot
N_samples = 8192;
dt = 8.138e-11;
t_start = 0;
df =1/(N_samples*dt);
V = complex(Sav, Sqav);
f = [0:1:(N_samples)/2-1,-(N_samples+1)/2:1:-1]*df;%sets the range doma
plot (f, abs(ifft(V,p)));
figure
```

The first plot shows the range profile before zero padding. The second plot shows the same figure after zero padding .

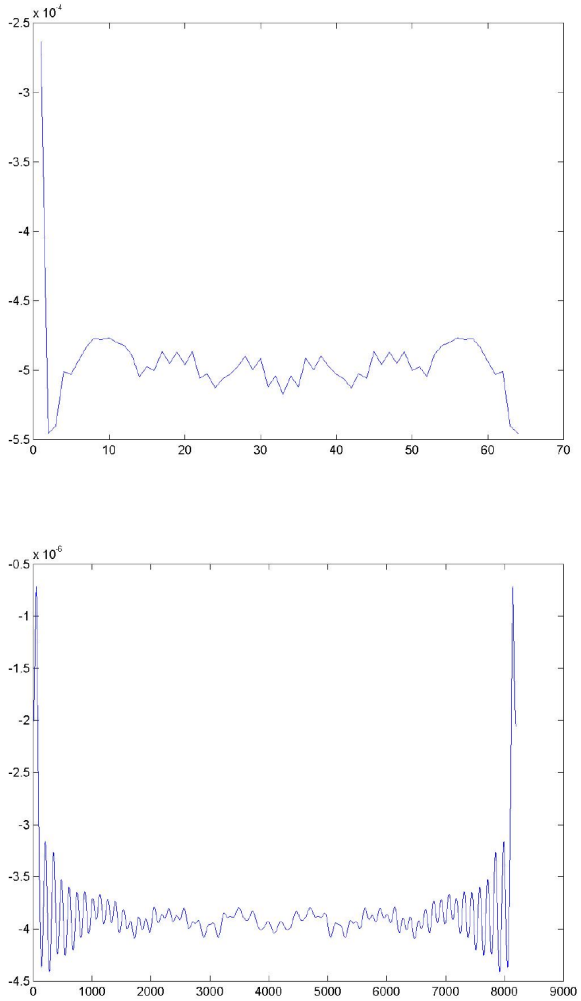

(a)

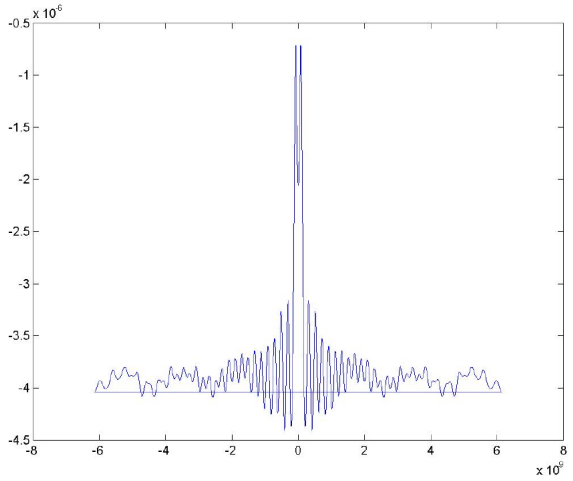

(b)

Figure C.1: Range profiles for the comparison system showing before zero padding and after zero padding.

Zero padding was done onto the 64 frequencies in order to smooth the range profile plot. The plot had sharp corners without zero padding. Thus it was very important that zero padding be implemented. The concept of zero padding comes from the relationship between the number of frequency steps and the range resolution. For a SFCW GPR with *n* = 64 and $\Delta f = 1.5MHz$, and bandwidth of 100 MHz transmitted for 20 ms. Each frequency is transmitted for 312.5 microseconds. Without zero padding or adding extra samples, the same time spacing would apply to the range profile in the time domain. This will not lead to HRR, 312.5 IS > 10 ns.The IFFT of the 64 frequency steps leads to a time domain profile with a two way time resolution of 10 nanoseconds.This is the ability to resolve between two targets separated by a time t seconds.Nw zero padding adds extra samples in the time domain, which makes high range resolution possible. With zero padding the samples are separated by a very small time interval, and thus can resolve targets separated by small time space. That is, targets separated by a small amount t will be resolved because there are more samples taken in the time plot. As the number of frequency steps increases, the range resolution alos becomes better.